

IAEA REPORT 2007

NEUTRONICS DESIGN OF THE FBNR

Submitted to the
INTERNATIONAL ATOMIC ENERGY AGENCY

Principal investigator
Farhang Sefidvash

Collaborator
Robson Silva da Silva

Federal University of Rio Grande do Sul,
Porto Alegre, Brazil

<http://www.rccg.urfgs.br/fbnr.htm>
farhang@sefidvash.net

Content

1.	Introduction.....	3
2.	Reactor description	3
3.	Fuel element description.....	7
4.	SCALE computational codes	8
5.	Cell calculations	9
5.1	CERMET Cell Calculations	9
5.2	Cell Description with TRISO Fuel	10
6.	Benchmarking with CERMET fuel.....	13
6.1	TRISO Unit Cell.....	13
6.2	Burnup with CERMET Fuel.....	14
7.	Standard FBNR Calculations	15
7.1	Contribution of each reactor part.....	17
7.2	Reactivity due to core height, enrichment and Boron concentration.	19
7.3	Sensitivity of reactivity to reactor height	20
7.4	Moderator temperature coefficient	23
7.5	Doppler Effect	24
7.6	Moderator Density	25
8.	Burnup Calculations.....	27
8.1	Burnup calculations.....	27
9.	Reactor operation and safety	30
9.1	Reactor start up and shut down	30
9.2	Reactor Safety: Accident Conditions	31
9.2.1	The Loss of Coolant Accident (LOCA)	31
9.2.2	The Loss of Flow Accident (LOFA).....	31
9.2.3	The Loss of Power Accident	31
9.2.4	The Loss of Turbine Load or Secondary Loop Break Accident	31
9.2.5	The Terrorist Attack	32
10.	Plutonium Utilization	32
11.	Conclusions.....	34
12.	References	34
13.	Acknowledgement	35

1. Introduction

The Fixed Bed Nuclear Reactor (FBNR) is being developed under the IAEA Coordinated Research Project (CRP) on Small Reactors Without O-site Refueling (SRWOR) [IAEA Research Contract No. 12960/ Regular Budget Fund (RBF)].

The Small Reactors without On-Site Refuelling are defined by IAEA “As reactors which have a capability to operate without refuelling and reshuffling of fuel for a reasonably long period consistent with the plant economics and energy security, with no fresh and spent fuel being stored at the site outside the reactor during its service life. They also should ensure difficult unauthorized access to fuel during the whole period of its presence at the site and during transportation, and design provisions to facilitate the implementation of safeguards. In this context, the term “refuelling” is defined as the ‘removal and/or replacement of either fresh or spent, single or multiple, bare or inadequately confined nuclear fuel cluster(s) or fuel element(s) contained in the core of a nuclear reactor’. This definition does not include replacement of well-contained fuel cassette(s) in a manner that prohibits clandestine diversion of nuclear fuel material.”

The FBNR intended to be simple in design, modular, inherent safety, passive cooling, proliferation resistant, and reduced environmental impact.

2. Reactor description

The Fixed Bed Nuclear Reactor (FBNR) is a small reactor (70 MWe) without the need of on-site refueling. It utilizes the PWR technology. It has the characteristics of being simple in design, modular, inherent safety, passive cooling, proliferation resistant, and reduced environmental impact. Here, the neutronics analysis of this reactor concept is presented.

The FBNR fuel chamber is fuelled in the factory. The sealed fuel chamber is then transported to and from the site. The FBNR has a long fuel cycle time and there is no need for on-site refuelling. The reactor makes an extensive use of PWR technology. It is an integrated primary system design.

The reactor as shown in the schematic figure, have in its upper part the reactor core and a steam generator and in its lower part the fuel chamber. The core consists of two concentric perforated zircaloy tubes of 31 cm and 171 cm in diameters, inside which, during the reactor operation, the spherical fuel elements are held together by the coolant flow in a fixed bed configuration, forming a suspended core. The coolant flows vertically up into the inner perforated tube and then, passing horizontally through the fuel elements and the outer perforated tube, enters the outer shell where it flows up vertically to the steam generator. The reserve fuel chamber is a 60 cm diameter tube made of high neutron absorbing alloy, which is directly connected underneath the core tube. The fuel chamber consists of a helical 30 cm diameter tube flanged to the reserve fuel chamber that is sealed by the national and international authorities. A grid is provided at the lower part of the tube to hold the fuel elements within it. A steam generator of the shell-and-tube type is integrated in the upper part

of the module. A control rod can slide inside the centre of the core for fine reactivity adjustments. The reactor is provided with a pressurizer system to keep the coolant at a constant pressure. The pump circulates the coolant inside the reactor moving it up through the fuel chamber, the core, and the steam generator. Thereafter, the coolant flows back down to the pump through the concentric annular passage. At a flow velocity called terminal velocity, the water coolant carries the 15 mm diameter spherical fuel elements from the fuel chamber up into the core. A fixed suspended core is formed in the reactor. In the shut down condition, the suspended core breaks down and the fuel elements leave the core and fall back into the fuel chamber by the force of gravity. The fuel elements are made of UO_2 micro spheres embedded in zirconium and clad by zircaloy.

Any signal from any of the detectors, due to any initiating event, will cut-off power to the pump, causing the fuel elements to leave the core and fall back into the fuel chamber, where they remain in a highly subcritical and passively cooled conditions. The fuel chamber is cooled by natural convection transferring heat to the water in the tank housing the fuel chamber.

The pump circulates the water coolant in the loop and at the mass flow rate of about 220 kg/sec, corresponding to the terminal velocity of 1.50 m/sec in the reserve fuel chamber, carries the fuel elements into the core and forms a fixed bed. At the operating flow velocity of 7.23 m/sec, corresponding to the mass flow rate of 1060 kg/sec, the fuel elements are firmly held together by a pressure of 0.188 bars that exerts a force of 27.1 times its weight, thus forming a stable fixed bed. The fixed bed is compacted by a pressure of 1.3 bars. The coolant flows radially in the core and after absorbing heat from the fuel elements enters the integrated heat exchanger of tube and shell type. Thereafter, it circulates back into the pump and the fuel chamber. The long-term reactivity is supplied by fresh fuel addition and possibly aided by a fine control rod that moves in the center of the core controls the short-term reactivity. A piston type core limiter adjusts the core height and controls the amount of fuel elements that are permitted to enter the core from the reserve chamber. The control system is conceived to have the pump in the “not operating” condition and only operates when all the signals coming from the control detectors simultaneously indicate safe operation. Under any possible inadequate functioning of the reactor, the power does not reach the pump and the coolant flow stops causing the fuel elements to fall out of the core by the force of gravity and become stored in the passively cooled fuel chamber. The water flowing from an accumulator, which is controlled by a multi redundancy valve system, cools the fuel chamber functioning as the emergency core cooling system. The other components of the reactor are essentially the same as in a conventional pressurized water reactor.

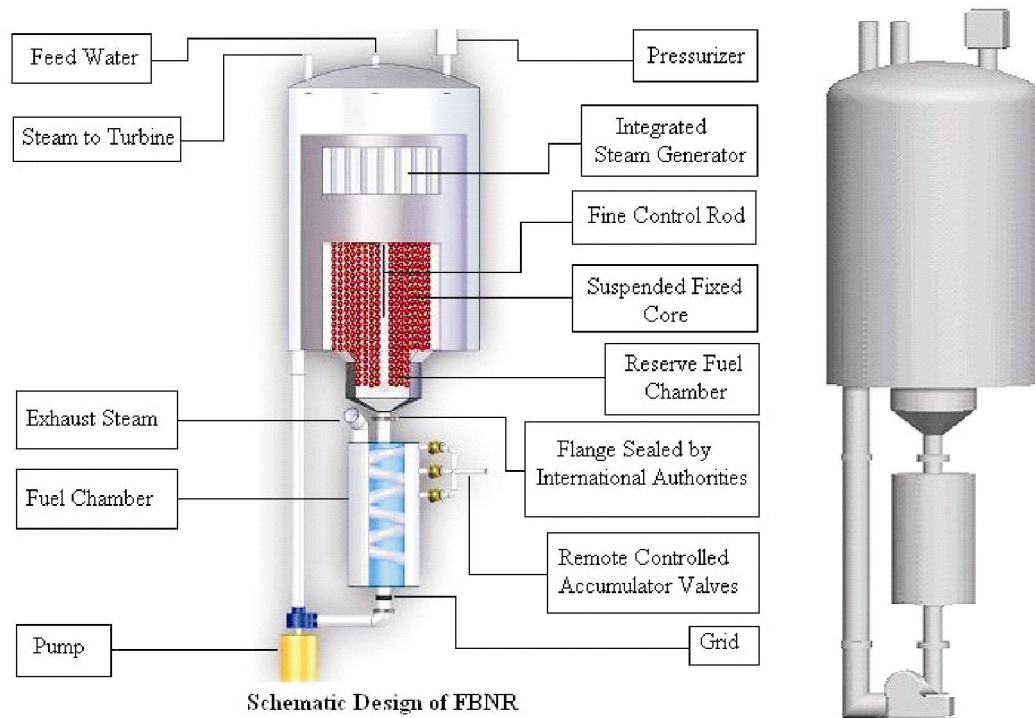


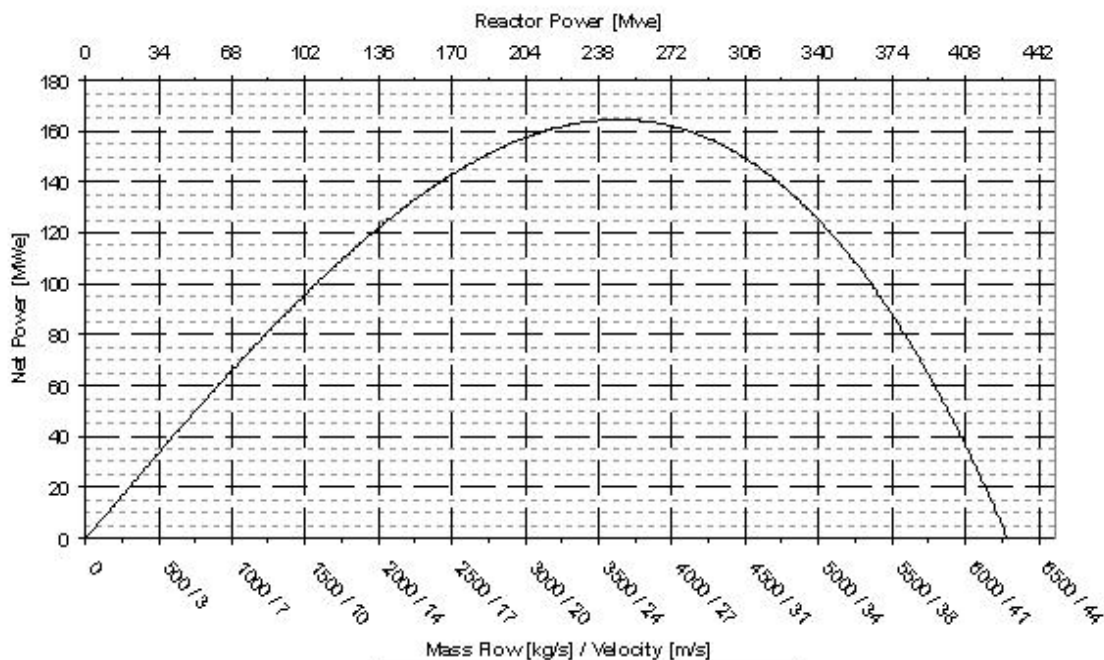
Figure 2.1: Schematic Design of FBNR

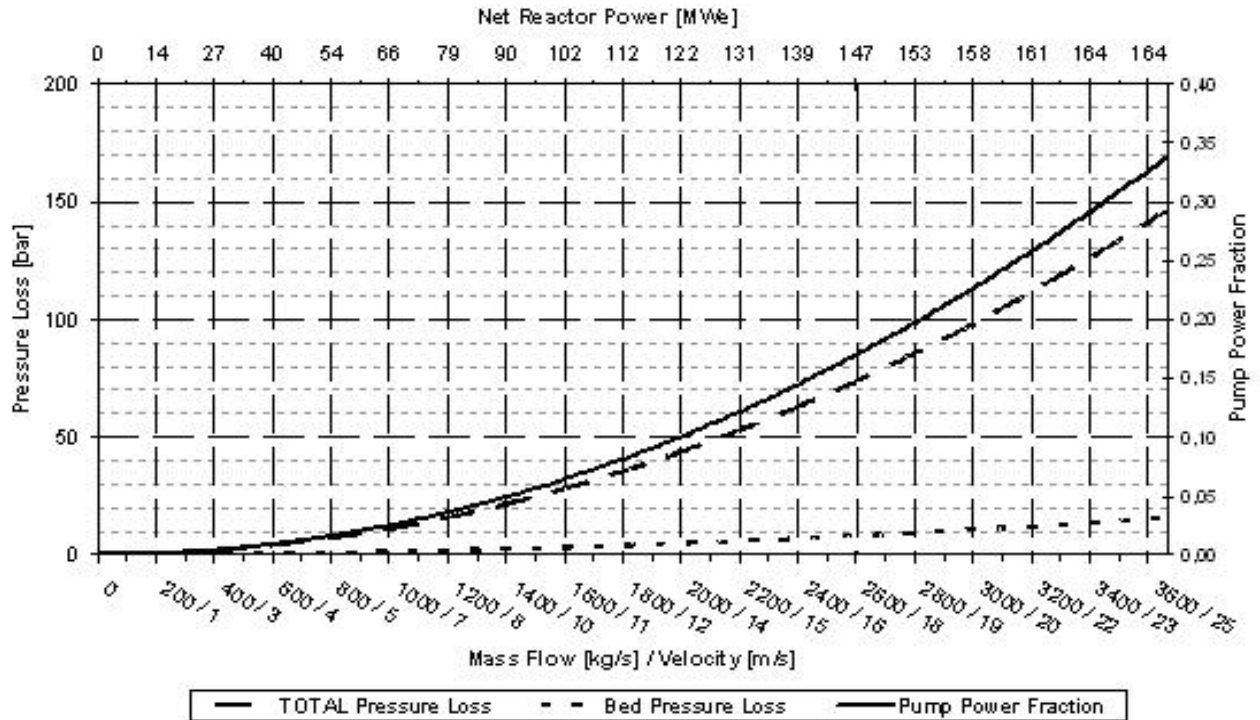
Table 2.1: Technical data for the Fixed Bed Nuclear Reactor (FBNR)

Parameter	Value	Parameter	Value
Power		Coolant temperature rise after a LOFA after 10 days ($^{\circ}\text{C}$)	< 1
Net power generation (MWe)	70	Water needed to cool during 10 days after LOCA (m^3)	0.9
Thermal power generation (MWt)	218	Neutronics	
Core power density (KWt/lit)	45.6	Moderator Coefficient ($\text{mK}/^{\circ}\text{C}$)-BOC	-3×10^{-4}
Pump power (MWe)	2	Moderator Coefficient ($\text{mK}/^{\circ}\text{C}$)-EOC	-8×10^{-4}
Pump power fraction (%)	2.8	Doppler Coefficient ($\text{mK}/^{\circ}\text{C}$) - BOC	-6×10^{-5}
Hydraulics		Doppler Coefficient ($\text{mK}/^{\circ}\text{C}$) - EOC	-7×10^{-5}
Coolant volume (m^3)	10	Core height level limiter (CHLL) Sensitivity (mK/cm) - BOC	0.37
Coolant mass flow (kg/sec)	1060	Core height level limiter (CHLL) Sensitivity (mK/cm) - EOC	0.059
Coolant pressure (bar)	160	Boron Sensitivity (mK/ppm) - BOC	0.039
Pressure loss in the loop (bar)	12.3	Boron Sensitivity (mK/ppm) - EOC	0.080
Pressure loss in the bed (bar)	1.3	Fuel Burnup [MWD/T / Years]	15300 / 2.2
Terminal velocity (m/sec)	1.5	Plutonium Production (Kg)	62
Operating coolant velocity (m/sec)	7.23	Remaining U-235 (Kg)	340

Thermal	
Coolant inlet temperature (°C)	290
Coolant outlet temperature (°C)	326
Coolant average temperature (°C)	308
Fuel operating temperature (°C)	354
Coolant inlet enthalpy (kJ/kg)	1284
Coolant inlet density (kg/m ³)	747
Coolant average density (Kg/m ³)	710
Enthalpy rise in the core (kJ/kg)	1490
Film boiling convective heat transfer coefficient at 300 °C (W/m ² °C)	454
Fuel element average thermal conductivity (W/m.°C)	12.5
Thermal conductivity Zirconium (W/m. °C)	18
Thermal conductivity Uranian Dioxide (W/m. °C)	7
Fuel element average specific heat (J/kg.°C)	
Fuel element average density (gr/cm ³)	8.09
Maximum fuel temperature after a LOCA (°C)	542

Core dimensions	
Core height (cm)	200
Core inner diameter (cm)	31
Core outer diameter (cm)	171
Core volume (m ³)	4.78
Fuel Element in the core (Ton)	23.2
UO2 in the core (Ton)	11.5
Fuel element	
Fuel element diameter (cm)	1.5
Zircaloy clad thickness (cm)	0.03
Number of fuel elements in the core.	1.62x10 ⁶
UO2 in each fuel element (% vol)	23.9
UO2 density (gr/cm ³)	10.5
Zirconium (gr/cm ³)	6.5





3. Fuel element description

The CERMET fuel is proposed for the FBNR reactor. The fuel consists of coated UO₂ kernels embedded in a zirconium matrix which is then coated with a protective outer zirconium layer. CERMET Fuels have significant potential to enhance fuel performance because of low internal fuel temperatures and low stored energy. The combination of these benefits with the inherent proliferation resistance, high burnup capability, and favourable neutronic properties of the thorium fuel cycle produces intriguing options for using thorium based cermet nuclear fuel in advanced nuclear fuel cycles.

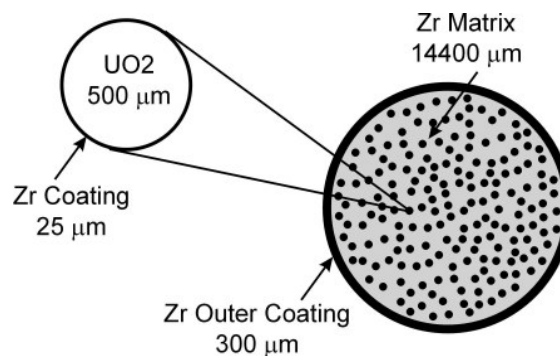


Figure 3.1: Cermet Unit Cell

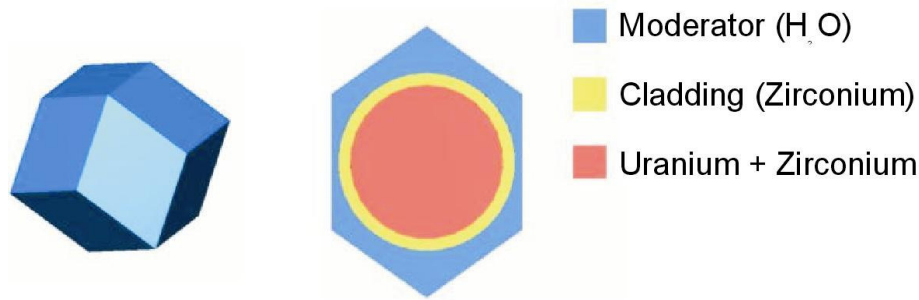


Figure 3.2 : CERMET Unit Cell

4. SCALE computational codes

SCALE (Standardized Computer Analyses for Licensing Evaluation) is a modular code system that was originally developed by Oak Ridge National Laboratory (ORNL).. The SCALE system utilizes well-established computer codes and methods within standard analysis sequences that:

- (1) provide an input format designed for the occasional user and/or novice,
- (2) automate the data processing and coupling between modules, and
- (3) provide accurate and reliable results.

System development has been directed at problem dependent cross-section processing and analysis of criticality safety, shielding, depletion/decay, and heat transfer problems.

Criticality Safety Analysis Sequence (CSAS) was developed to provide a search capability for three-dimensional (3-D) configurations in the SCALE system. At the center of the Criticality Safety Analysis Sequences (CSAS) is the library of subroutines referred to as the **Material Information Processor Library** or MIPLIB. The CSAS control module is the primary criticality safety control module for the calculation of the neutron multiplication factor of a system. Multiple sequences within the CSAS module provide capabilities for a number of analyses, such as modelling a one dimensional (1-D) or a 3-D system, searching on geometry spacing or material concentrations, and processing cross sections.

The 238-group ENDF/B-V library (238GROUPNDF5) is the most complete library in SCALE 5. This library contains data for all ENDF/B-V nuclides and has 148 fast and 90 thermal groups. The 238- and 44-group libraries are the preferred criticality safety analysis libraries in SCALE. The 44-group library is recommended for LWR systems, and the 238-group library is recommended for all other types of systems. The 238-group library was used in our calculations.

CSAS: control module for enhanced criticality safety analysis sequences has the following inherent limitations:

1. Double heterogeneity such as HTGR or Pebble Bed fuel, where uranium encased in small graphite spheres are used to make larger spheres or rods which are then placed in a regular lattice.

2. Two-dimensional (2-D) effects such as fuel rods in assemblies where some positions are filled with control rod guide tubes, burnable poison rods and/or fuel rods of different enrichments. The cross sections are processed as if the rods are in an infinite lattice of identical rods.

CSAS performs a search for 3-D problems. CSAS25 calculates the k_{eff} for 3-D problems. KENO V.a is a functional module in the SCALE system. It calculates the k_{eff} (*i.e.*, neutron multiplication) of a 3-D problem using the Monte Carlo methodology. A 238-energy-group neutron cross-section library based on ENDF/B-V2 is the latest cross-section library in SCALE. All the nuclides that are available in ENDF/B-V are in the library. A 44-group library has been collapsed from this 238-group library and validated against numerous critical measurements.

5. Cell calculations

5.1 CERMET Cell Calculations

Due to the computer code limitation, one fuel-element is divided into two regions: The inner region, consisting coated particles inside a zirconium matrix, is simulated as a homogenized mixture of these components. The mass fractions of each material are listed in Table 5.2..1. The outer region consists the 0.3 mm Zircaloy cladding.

To simulate the reactor as a cylinder, filled by fuel spheres and water, each fuel element is surrounded by a dodecahedral water region. Arranging several Dodecahedrons on each other allows modelling the reactor core. The radius of one dodecahedron is chosen as such, to get a porosity of 40% (volume-fraction of water to fuel). The composition of these 3 regions (Fuel, Zircaloy and Water) creates one fuel unit.

The input data to SCALE code calculations require the following information.

Table 5.1.1: Mixture of CERMET Unit Cell

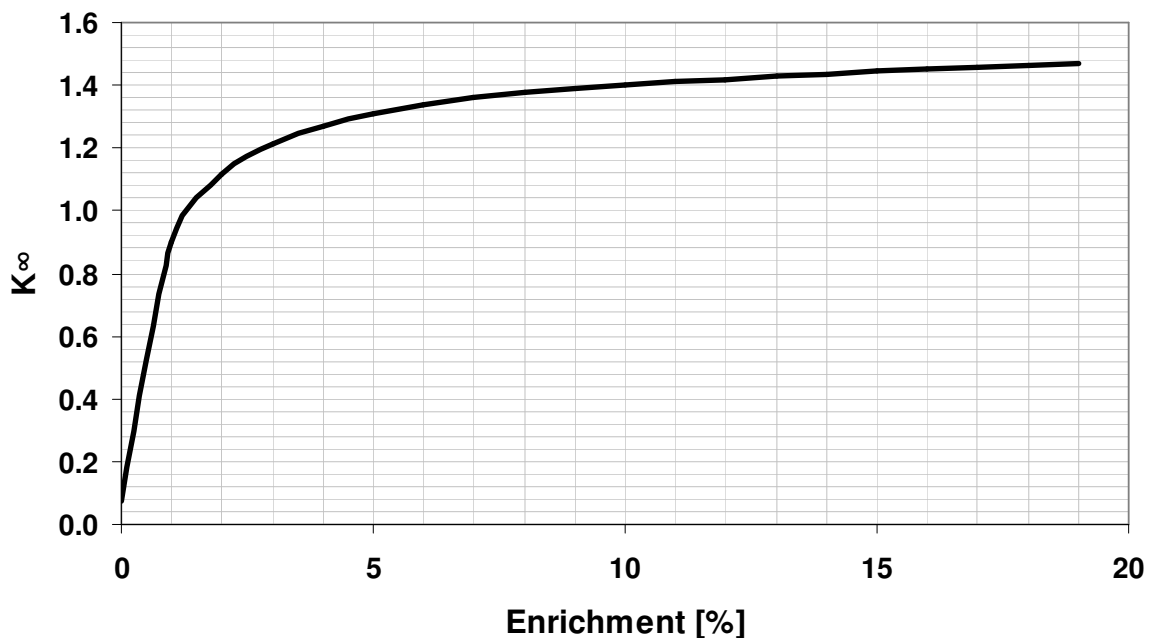
Material	Density (g/cc)	Diameter (cm)	Volume (cm ³)	Mass (gr)	Mass Fraction
UO ₂ in Fuel Element	10.5		0.705	7.402	0.570
Zirconium	6.5		0.858	5.577	0.430
Total	8.304	1.440	1.563	12.979	1
Cladding Zirconium	6.5	Thickness 0.03	0.204	1.324	
Fuel Element	8.09	1.5	1.767		
H ₂ O inside dodecaedron	0.747	Face to face 1.62	1.178	0.880	
Total Unit Cell	5.156		2.945	15.183	

The calculations were made for two boundary conditions: Mirror and Vacuum. A mirrored boundary condition will give the best possibility to simulate k_{∞} by using a single cell.

The for various fuel enrichment in a unit cell are shown in Table 5.1.2 and Fig. 5.1.1.

Table 5.1.2: K_{∞} as a function of enrichment for CERMET unit cell

Enrichment (%)	K_{eff}	Enrichment (%)	K_{eff}
0	0.0717	11	1.4129
1	0.9015	12	1.4196
2	1.1154	13	1.4296
3	1.2146	14	1.4373
4	1.2720	15	1.4449
5	1.3097	16	1.4502
6	1.3376	17	1.4591
7	1.3591	18	1.4654
8	1.3760	19	1.4696
9	1.3880	99	1.7906
10	1.4005		

Figure 5.1.1: K_{inf} as a function of enrichment for CERMET unit cell

5.2 Cell Description with TRISO Fuel

In the past the TRISO type microspheres were used in the FBNR reactor. There was raised a doubt about the behaviour of SiC in such a fuel with hot water in a radiation environment. To avoid such critics, it was decided to use CERMET fuel. Here the results of unit cell calculations for TRISO and CERMET fuels are compared.

A description of fuel element with TRISO type fuel are as follows: The 15 mm diameter spherical fuel elements are made of compacted coated particles in a graphite matrix. The coated particles are similar to TRISO fuel with outer diameters about 2mm. They consist of 1.58 mm diameter uranium dioxide spheres coated with 3 layers. The inner layer is of 0.09 mm thick porous pyrolytic carbide (PYC) with density of 1 g/cm³ called buffer layer,

providing space for gaseous fission products. The second layer is of 0.02 mm thick dense PYC (density of 1.8 g/cm³) and the outer layer is 0.1 mm thick corrosion resistant silicon carbide (SiC, density of 3.17 g/cm³). The fuel element is clad by 1mm thick SiC.

Table 5.2.1: Fuel particle (2 mm diameter)

Material	density (g/cm ³)	d. inside (cm)	d.outside (cm)	volume (cm ³)	mass (gr)
UO ₂	10.50	0	0.158	0.00206	0.02168
PYC (porous)	1.00	0.158	0.176	0.00078	0.00078
PYC (dense)	1.80	0.176	0.180	0.00019	0.00035
SiC	3.17	0.18	0.2	0.00113	0.00359
Average for microsphere	6.31		0.2	0.00418	0.02643

The volume fractions of each material are listed in Table 5.2..2. The outer region consists the 1mm SiC cladding.

Table 5.2.2: Mixture of Region 1

Material	Mass (gr)	Volume (cm ³)	Density (g/cm ³)	Mass fraction	Volume fraction	Thermal conductivity (W/m. °C)	Specific heat (kJ/kg. °C)
UO ₂	3.578	0.341	10.5	0.501	0.193	5.2	
PYC porous (amorfo) 600K	0.130	0.130	1.00	0.0182	0.0737	2.19	1406
PYC dense (amorfo) 600K	0.887	0.493	1.80	0.124	0.279	2.19	1406
SiC	2.549	0.804	3.17	0.357	0,455	77.5	1300
fuel element	7.145	1.768	4.04	1	1	30.566	1400

To simulate the reactor as a cylinder, filled by fuel spheres and water, each fuel element is surrounded by a dodecahedron water region. Arranging several Dodecahedrons on each other allows modelling the reactor core. The radius of one dodecahedron is chosen as such, to get a porosity of 40% (volume-fraction of water to fuel). The composition of these 3 regions (Fuel, SiC, and Water) creates one fuel unit.

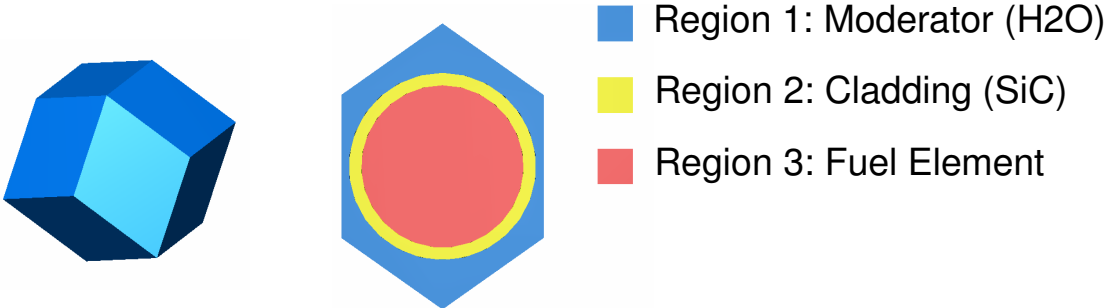


Figure 5.2.1: TRISO Unit cell

The reactivity as a function of enrichment for a single sphere was calculated. In case of the single cell, the values approach those of K_{∞} . The results are shown in Figure 5.2.2.

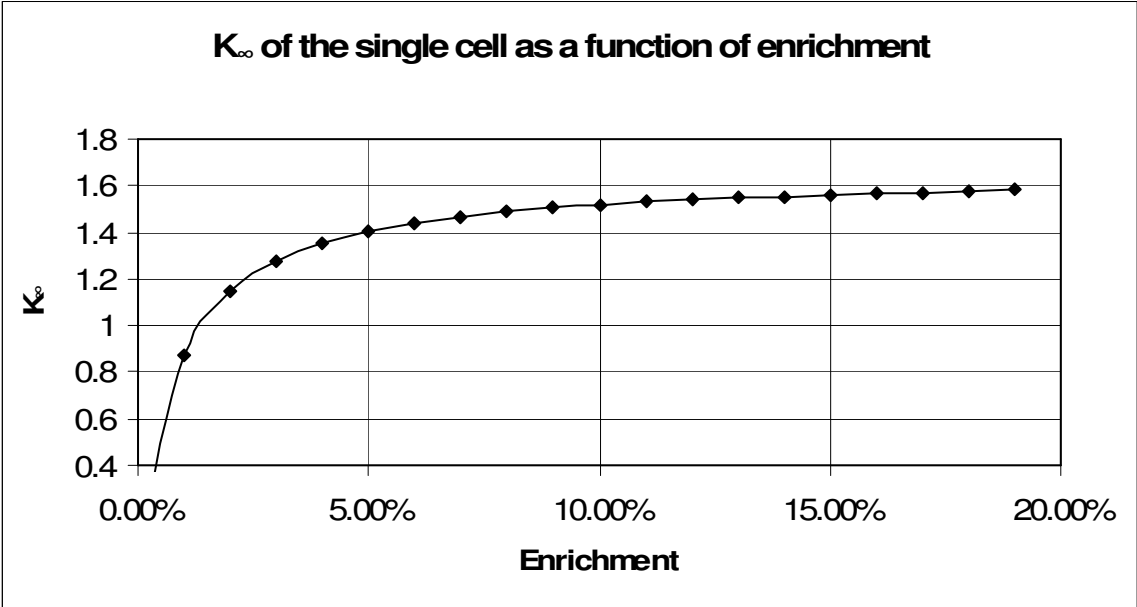


Figure 5.2.2: K_{∞} for a TRISO single cell

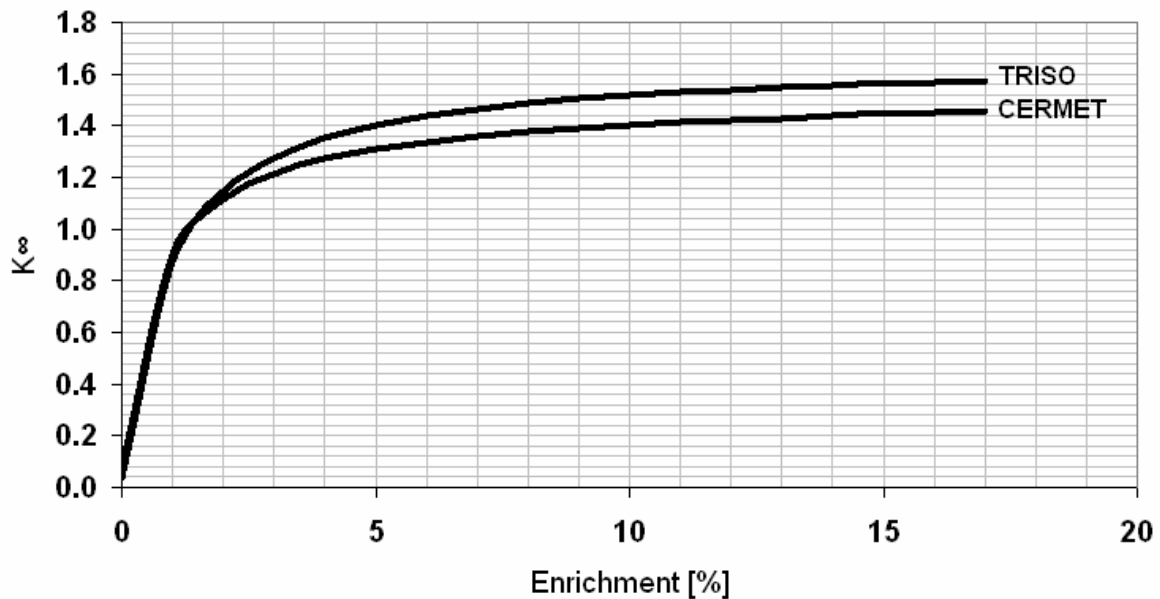


Figure 5.2.3: CERMET vs. TRISO

Up to an enrichment of 5%, k_{∞} increases considerably. After that point, k_{∞} rises moderately up to the maximum of 1,79 for an enrichment of 99%. The reactivity for maximum hypothetical enrichment is investigated. k_{∞} will be around 1.79 for a water moderated reactor and 1.82 for a graphite moderated reactor.

In table 5.2.3 the K_{∞} of a unit cell of CERMET fuel is compared to that of TRISO fuel of a 5% fuel enrichment. It seems that the neutron spectrum of cermet fuel is harder than that of the TRISO fuel.

Table 5.2.3: Unit cell (5% enrichment)

Mirror Boundary condition	K_{∞}
TRISO Fuel	1.40319
CERMET Fuel	1.30970

6. Benchmarking with CERMET fuel

6.1 TRISO Unit Cell

Takashi Hirayama [5] compared the K_{inf} calculated by various reactor codes for various reactor concepts using TRISO fuel. Table 6.1.1 shows the comparison of k -infinities at BOL by SRAC95, APOLLO and Monte Carlo calculation code MCNP⁷⁾, respectively. The MCNP code uses nuclear data library ENDF/B6. In the same table, the ratios of k -infinities by SRAC95 and APOLLO to those by MCNP are shown.

Table 6.1.1: The comparison of the k-infinity in BOL with Monte Carlo

	AFPR	AFPR-SC	BWR-PB	FBNR	PFWR50
SRAC95	1.15699	1.22671	1.50010	1.40546	1.29230
SRAC95/MCNP	1.02379	1.01172	0.99516	1.01153	0.99126
APOLLO	1.12605	1.22685	1.48610	1.38650	1.29074
APOLLO/MCNP	0.99642	1.01184	0.98588	0.99788	0.99006
MCNP	1.13010	1.21250	1.50739	1.38944	1.30370

6.2 Burnup with CERMET Fuel.

The K_e for FBNR40 version reactor (40 MWe), calculated by different codes gave the following results: SCALE = 1.1822; APOLLO = 1.2365; HAMMER/WIMS/ CITATION = 1.20718. The results of the burnup calculations for FBNR40 using SCALE and APOLLO are given in table 6.2.2.

Table 6.2.2: SCALE versus APOLLO burnup calculations

Days	MWD/Ton	SCALEFBNR40	APOLLOFBNR40	APOLLOFBNR40 divide by SCALEFBNR40
0	0.00	1.1822	1.2365	1.0459
1	13.79	1.1621	1.2220	1.0515
2	27.57	1.1597	1.2210	1.0529
3	41.36	1.1579	1.2206	1.0541
4	55.15	1.1571	1.2203	1.0546
5	68.94	1.1581	1.2199	1.0534
6	82.72	1.1583	1.2195	1.0528
7	96.51	1.1563	1.2191	1.0543
8	110.30	1.1564	1.2188	1.0540
9	124.08	1.1548	1.2184	1.0551
10	137.87	1.1560	1.2181	1.0537
120	1654.44	1.1389	1.1978	1.0517
240	3308.88	1.1205	1.1809	1.0539
360	4963.32	1.1023	1.1638	1.0558
480	6617.76	1.0896	1.1469	1.0526
600	8272.20	1.0695	1.1306	1.0571
720	9926.64	1.0566	1.1151	1.0554
840	11581.08	1.0425	1.1004	1.0555
960	13235.52	1.0267	1.0863	1.0581
1080	14889.96	1.0124	1.0729	1.0598
1200	16544.40	0.9970	1.0600	1.0632
1320	18198.84	0.9841	1.0477	1.0646
1440	19853.28	0.9716	1.0358	1.0661
1560	21507.72	0.9585	1.0242	1.0685
1680	23162.16	0.9451	1.0131	1.0720
1800	24816.60	0.9331	1.0022	1.0741
1920	26471.04	0.9199	0.9916	1.0779

2040	28125.48	0.9095	0.9813	1.0789
2160	29779.92	0.8983	0.9712	1.0812
2200	30331.40	0.8936	0.9679	1.0831

The K_e of standard FBNR40 reactor with cermet fuel are shown in table 6.2.2. Standard reactor is defined to have 200 cm core height and 5% fuel enrichment.

7. Standard FBNR Calculations

The code SCALE does not permit the treatment of double heterogeneity. For present studies, the objective being the study of the behavior of the reactor, the homogeneous calculations were considered sufficiently adequate. The homogeneous mixture at the fuel region consists of UO_2 , H_2O , and Zircaloy. The volume fractions of each material inside this region are listed in Table 7.1. The standard reactor having 200 cm core height and 5% fuel enrichment producing 218 MWt (70 MWe).

Table 7.1: Mixture of homogeneous Reactor for CERMET Fuel

	Mass Fraction	Density [g/cm ³]
Core material		
UO_2	0.48726	10.50
Zirconium	0.45480	6.50
H_2O	0.05794	0.747
Total	1	5.156
Moderator material		
H_2O		0.747
Structural material		
Stainless Steel SS-304		7.49
Zircaloy		6.56
Absorber material (lower Part)		
Cadmium		8.642

Figures 7.1, 7.2, 7.3, 7.4 show the homogenous model of the reactor, as it was used for the k_{eff} and burnup calculations.

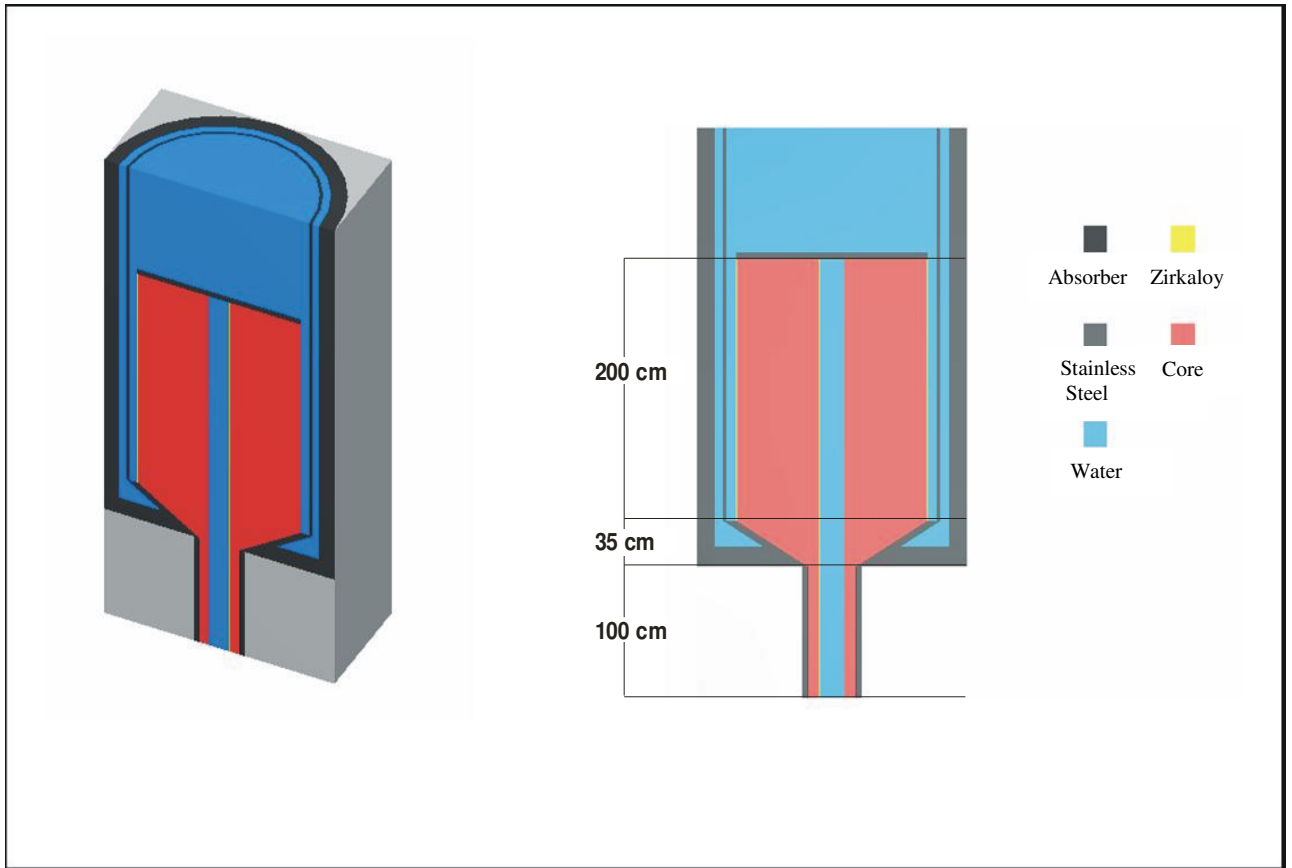


Figure 7.1: Keno VI model of homogenous reactor

Transversal sections of the upper part, middle part and lower part of the reactor are shown below:

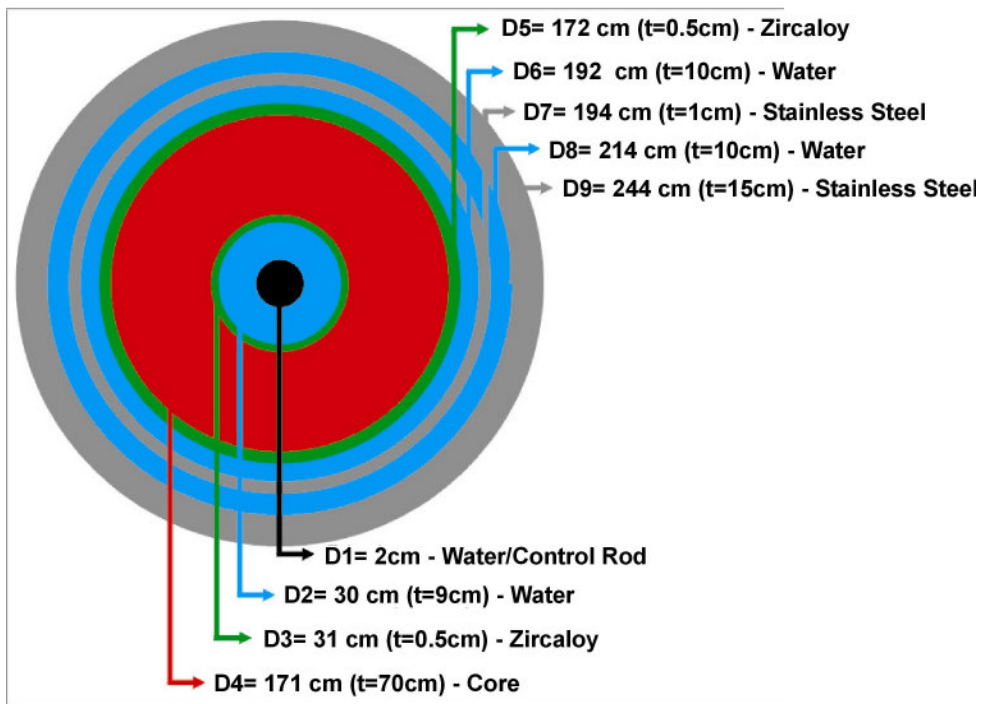


Figure 7.2: Upper Part

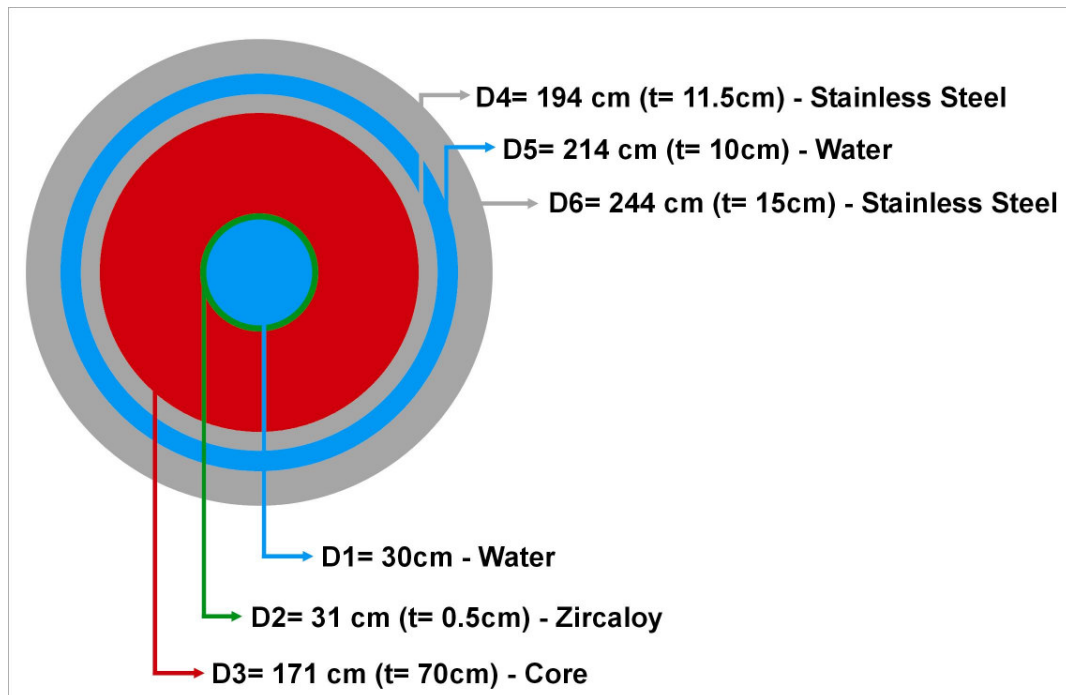


Figure 7.3: Middle Part

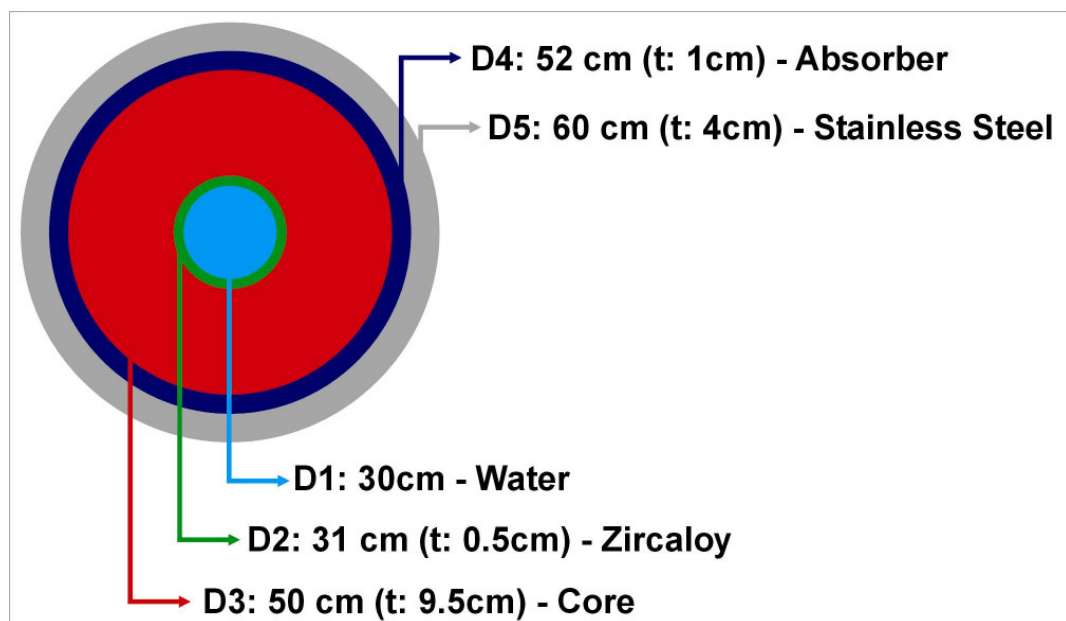


Figure 7.4: Lower Part

7.1 Contribution of each reactor part

The contributions of each part of the reactor core to the reactivity are shown in table 7.1.1 for cold and hot reactor. The upper cylindrical part, the middle conical part, and the lower cylindrical part are made full or empty of fuel elements and its vessels are assumed to be made of a neutron absorber or conventional steel.

Table 7.1.1: Contribution of each reactor part

	Temperature 20°C	Temperature 327°C
- Upper part without fuel - Middle part with fuel without absorber - Lower Part with fuel and with absorber	Ke = 0.96250	Ke = 0.85290
- Upper part without fuel - Middle part with fuel and with absorber - Lower Part with fuel and with absorber	Ke = 0.92536	Ke = 0.81568
- Upper part without fuel - Middle part without fuel and without absorber - Lower Part with fuel and with absorber	Ke = 0.63478	Ke = 0.60791
- Upper part without fuel - Middle part without fuel and without absorber - Lower Part with fuel and without absorber	Ke = 0.67732	Ke = 0.64947

The Ke for the standard reactor with soluble boron in cold and hot conditions are given in table 7.1.2 and fig. 7.1.1.

Table 7.1.2: Ke as a function of boron concentration for cold and hot reactor

Boron Concentration (ppm)	Ke	
	327 °C	20 °C
0000	1.17370	1.26240
1000	1.08770	1.15610
2000	1.03580	1.09560
3000	0.99361	1.02281
4000	0.94954	0.97364
5000	0.90852	0.92178

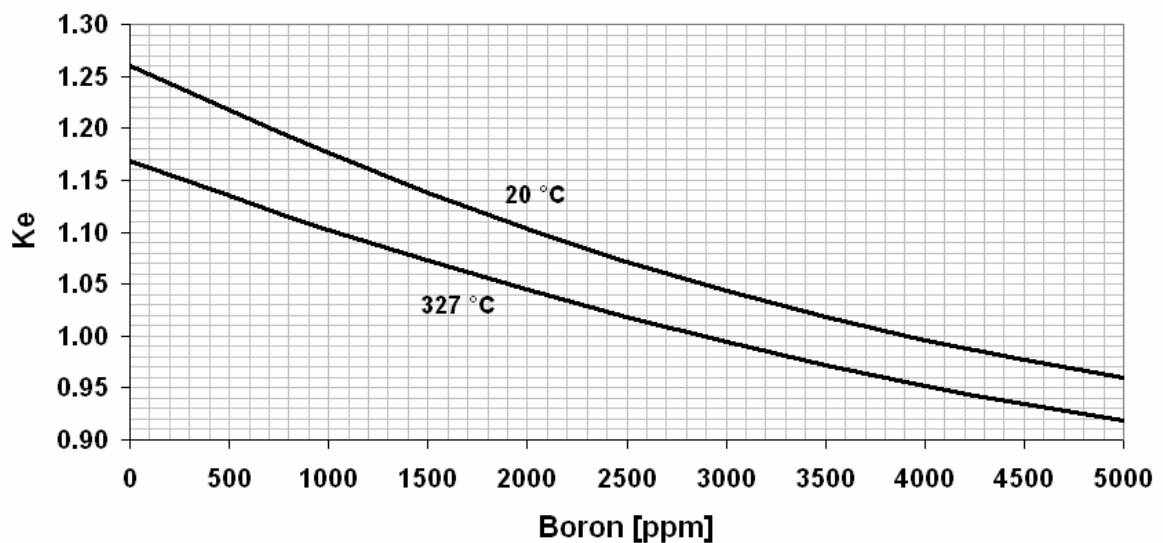


Fig. 7.1.1: Ke as a function of Boron concentration for cold and hot reactor.

The results of the reactivity as a function of boron concentration can be fitted to the following equations. It is deduced that the hot reactor with 2880 ppm and cold reactor with 3900 ppm Boron concentrations are critical.

$$\text{for } 20^{\circ}\text{C, } K_e = 6 \times 10^{-9} x^2 - 9 \times 10^{-5} x + 1.2599$$

and

$$\text{for } 327^{\circ}\text{C, } K_e = 4 \times 10^{-9} x^2 - 7 \times 10^{-5} x + 1.1684$$

where x is boron concentration in ppm. Therefore, the boron concentration of 2900 ppm was chosen for the beginning of cycle.

7.2 Reactivity due to core height, enrichment and Boron concentration.

The global neutron multiplication factor of the reactor as a function of core height for various boron concentration of 0, 1000, 2000 and 3000 ppm are shown in Table 7.2.1 and Figure 7.2.1.

It is seen that the height up to about 120 cm, the core height has a significant influence on reactivity. At higher values the sensitivity is small. This helps the reactivity control by movement of core height level limiter (CHLL) without the need of having fine control rods.. However, there is a need to use Boron poison to reduce k_{eff} at the beginning of the burnup cycle. The K_e as a function of the core height and boron concentrations are shown in table 7.2.1 and fig 7.2.1.

Table 7.2.1: K_e as a function of the core height and boron concentration

Height	0 ppm	1000 ppm	2000 ppm	3000 ppm
0	0.85190	0.78370	0.73750	0.70880
10	0.93510	0.87020	0.82580	0.78930
20	0.99780	0.92840	0.88230	0.84570
30	1.04150	0.97220	0.92054	0.88470
40	1.07260	0.99940	0.94877	0.91160
50	1.09470	1.02170	0.96920	0.92980
60	1.11170	1.03650	0.98260	0.94320
70	1.12370	1.05000	0.99479	0.95450
80	1.13130	1.05698	1.00140	0.96230
90	1.14120	1.06543	1.00960	0.96720
100	1.14708	1.07080	1.01500	0.97080
110	1.15270	1.07430	1.02160	0.97709
120	1.15570	1.08092	1.02250	0.98080
130	1.15970	1.08390	1.02650	0.98350
140	1.16290	1.08535	1.02880	0.98500
150	1.16450	1.08639	1.02830	0.98852
160	1.16630	1.08940	1.03117	0.99100
170	1.16860	1.09090	1.03500	0.99100
180	1.16940	1.09500	1.03490	0.99383
190	1.17060	1.09240	1.03640	0.99410
200	1.17370	1.09434	1.03690	0.99381
210	1.17450	1.09660	1.03869	0.99569
220	1.17760	1.09807	1.03950	0.99690
230	1.17460	1.09537	1.04030	0.99780
240	1.17750	1.09690	1.04020	0.99553
250	1.17760	1.10110	1.04023	0.99807

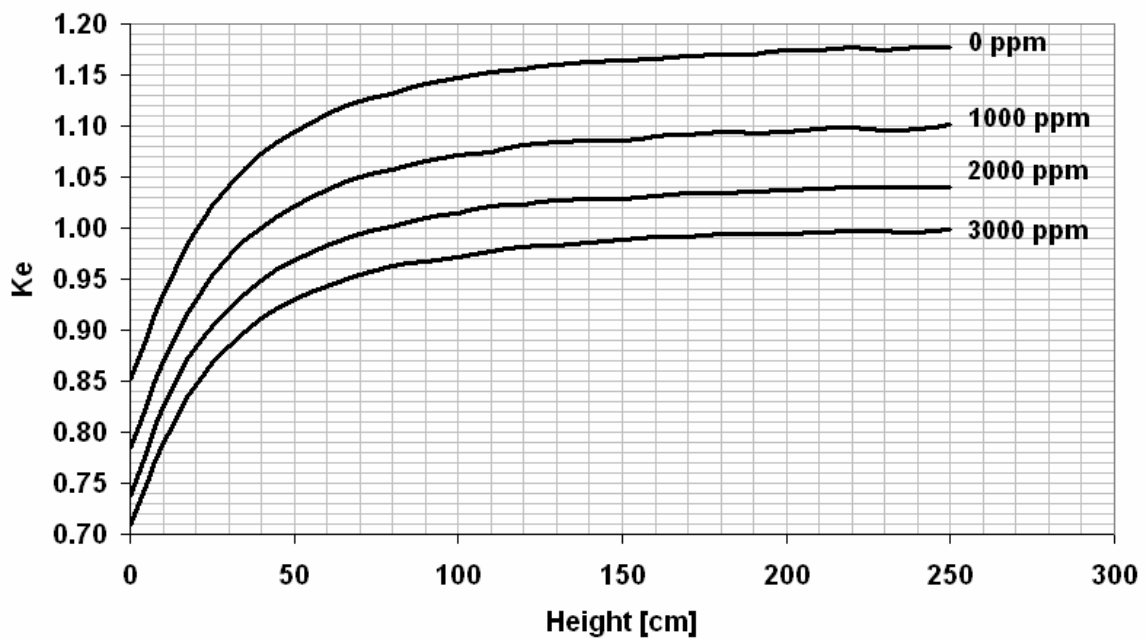


Figure 7.2.1: K_e as a function of the core height and boron concentration

7.3 Sensitivity of reactivity to reactor height

The short term reactivity control is done by changing the reactor height by the core height level limiter (CHLL). Therefore, the sensitivity of the reactivity to core height needs to be known. The K_e as a function of core height (x) has been fitted to a polynomial of tenth degrees resulting in.

0 ppm Boron:

$$ke = 0.85183 + 9.5461 \times 10^{-3} x - 1.2134 \times 10^{-4} x^2 + 9.6395 \times 10^{-8} x^3 + 1.9588 \times 10^{-8} x^4 - 3.045 \times 10^{-10} x^5 + 2.4183 \times 10^{-12} x^6 - 1.169 \times 10^{-14} x^7 + 3.5026 \times 10^{-17} x^8 - 6.0394 \times 10^{-20} x^9 + 4.605 \times 10^{-23} x^{10}$$

1000 ppm Boron:

$$ke = 0.78375 + 1.0319 \times 10^{-2} x - 1.9355 \times 10^{-4} x^2 + 2.4669 \times 10^{-6} x^3 - 2.1759 \times 10^{-8} x^4 + 1.2337 \times 10^{-10} x^5 - 3.1314 \times 10^{-13} x^6 - 9.732 \times 10^{-16} x^7 + 1.0471 \times 10^{-17} x^8 - 3.179 \times 10^{-20} x^9 + 3.478 \times 10^{-23} x^{10}$$

2000 ppm Boron:

$$ke = 0.73758 + 1.1042 \times 10^{-2} x - 2.7224 \times 10^{-4} x^2 + 5.5238 \times 10^{-6} x^3 - 8.8605 \times 10^{-8} x^4 + 1.0326 \times 10^{-9} x^5 - 8.2382 \times 10^{-12} x^6 + 4.3133 \times 10^{-14} x^7 - 1.4066 \times 10^{-16} x^8 + 2.5813 \times 10^{-19} x^9 - 2.0319 \times 10^{-22} x^{10}$$

3000 ppm Boron:

$$ke = 0.70882 + 9.3609 \times 10^{-3} x - 1.3515 \times 10^{-4} x^2 - 4.6776 \times 10^{-8} x^3 + 3.9025 \times 10^{-8} x^4 - 7.5193 \times 10^{-10} x^5 \\ + 7.4973 \times 10^{-12} x^6 - 4.4464 \times 10^{-14} x^7 + 1.5726 \times 10^{-16} x^8 - 3.0617 \times 10^{-19} x^9 + 2.525 \times 10^{-22} x^{10}$$

Where, x = core height in centimeters.

The sensitivity of the reactivity to height being the derivative of above functions (dKe/dH) are evaluated and presented in table 7.3.1. and fig.7.3.1. It is seen that the sensitivity of reactivity to core height is almost independent of boron concentration.

Table 7.3.1: Sensitivity of reactivity to core height

Height	d(mk)/dH 0 ppm	d(mk)/dH 1000 ppm	d(mk)/dH 2000 ppm	d(mk)/dH 3000 ppm
0	9.54610	10.31900	11.04200	9.36090
10	7.21272	7.10701	6.94690	6.76657
20	5.23293	4.93334	4.63145	4.67159
30	3.70696	3.46734	3.23040	3.18695
40	2.61162	2.47660	2.31693	2.21027
50	1.86774	1.80293	1.69145	1.58412
60	1.38151	1.34123	1.25841	1.17251
70	1.06729	1.02236	0.96216	0.88587
80	0.85785	0.80016	0.75988	0.67759
90	0.70666	0.64278	0.61491	0.52856
100	0.58579	0.52734	0.49880	0.43032
110	0.48172	0.43739	0.39479	0.37324
120	0.39079	0.36203	0.29868	0.34181
130	0.31500	0.29571	0.21594	0.31663
140	0.25871	0.23788	0.15580	0.28068
150	0.22614	0.19165	0.12430	0.22618
160	0.21956	0.16140	0.11904	0.15860
170	0.23794	0.14932	0.12773	0.09498
180	0.27606	0.15179	0.13211	0.05528
190	0.32434	0.15709	0.11679	0.04860
200	0.37014	0.14684	0.08040	0.05898
210	0.40194	0.10463	0.04297	0.04071
220	0.41863	0.03621	0.03994	-0.06221
230	0.44712	0.00722	0.08809	-0.25114
240	0.57260	0.20531	0.10385	-0.33382
250	0.98715	1.03550	-0.25234	0.32497

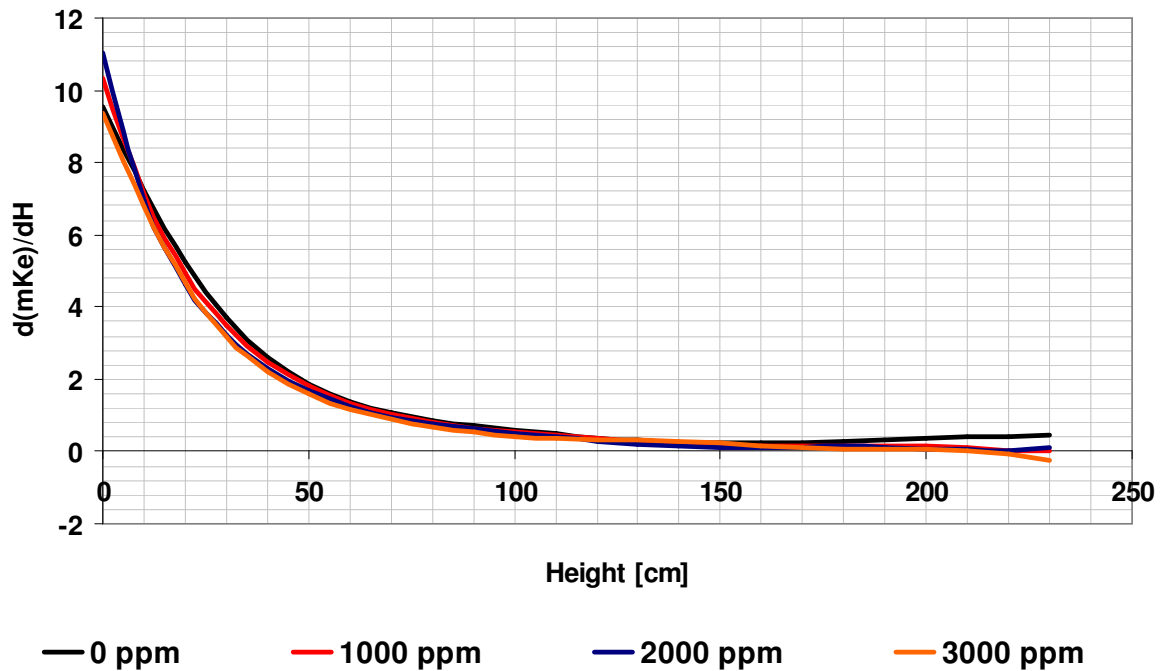


Figure 7.3.1: Sensitivity of reactivity to core height

The reactivity as a function of boron concentration are calculated for every 100 ppm interval. For the reason of computing time constrain, 500 iterations were used for the calculations. This fact caused some deviations in the results of the calculations. Therefore, to obtain a smooth curve, the data were fitted a polynomial using least square error method. The results are shown in table 7.3.2 and fig. 7.3.2.

Table 7.3.2: Fitted Curve

ppm B	Ke	Fitting Values	d(mke0/dB)	ppm B	Ke	Fitting Values	d(mke0/dB)
0	1.17370	1.17010	-0.08000	1600	1.06390	1.06002	-0.05760
100	1.16150	1.16217	-0.07860	1700	1.05300	1.05433	-0.05620
200	1.15570	1.15438	-0.07720	1800	1.05420	1.04878	-0.05480
300	1.14590	1.14673	-0.07580	1900	1.04626	1.04337	-0.05340
400	1.14050	1.13922	-0.07440	2000	1.03690	1.03810	-0.05200
500	1.12860	1.13185	-0.07300	2100	1.03705	1.03297	-0.05060
600	1.12840	1.12462	-0.07160	2200	1.02820	1.02798	-0.04920
700	1.11725	1.11753	-0.07020	2300	1.02890	1.02313	-0.04780
800	1.10490	1.11058	-0.06880	2400	1.01880	1.01842	-0.04640
900	1.10530	1.10377	-0.06740	2500	1.01114	1.01385	-0.04500
1000	1.09434	1.09710	-0.06600	2600	1.01274	1.00942	-0.04360
1100	1.09280	1.09057	-0.06460	2700	1.00039	1.00513	-0.04220
1200	1.08560	1.08418	-0.06320	2800	1.00300	1.00098	-0.04080
1300	1.07460	1.07793	-0.06180	2900	0.99519	0.99697	-0.03940
1400	1.07340	1.07182	-0.06040	3000	0.99381	0.99310	-0.03800
1500	1.06420	1.06585	-0.05900				

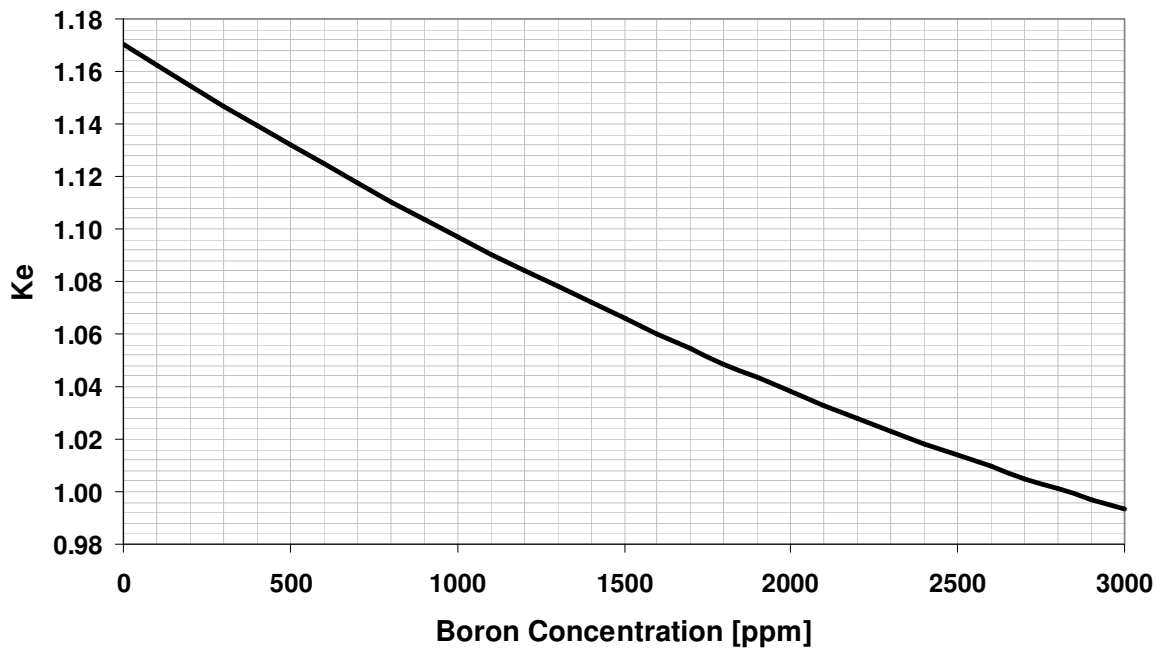


Figure 7.3.2: Reactivity as a function of boron concentration

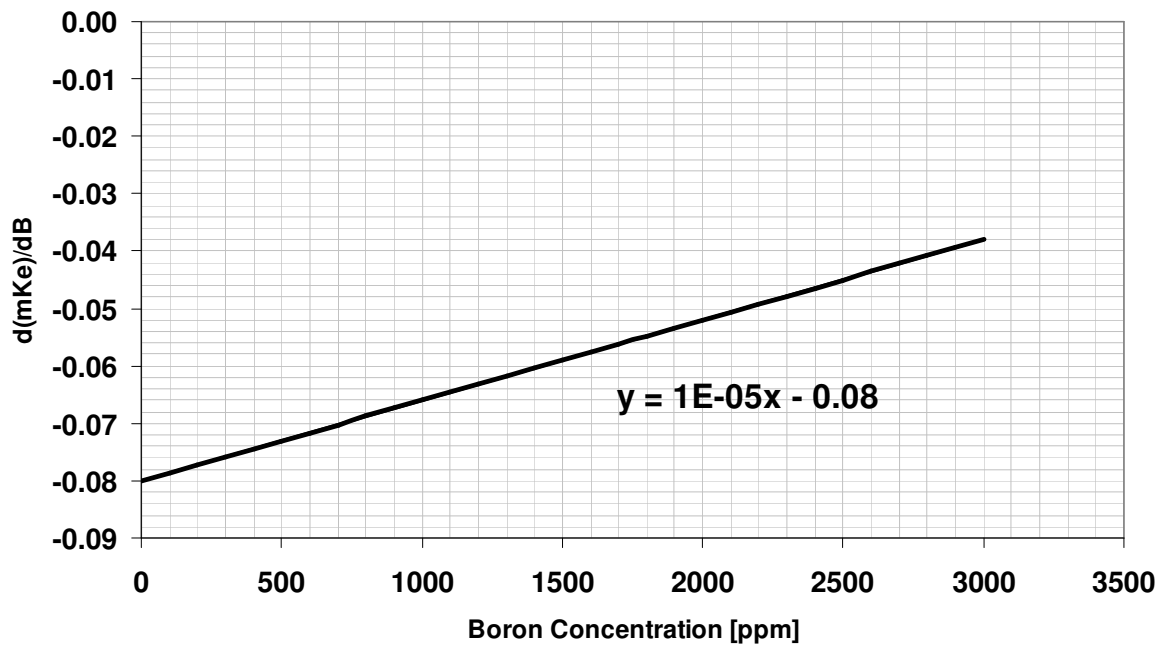


Figure 7.3.3: Sensitivity of the reactivity to boron concentration

7.4 Moderator temperature coefficient

The reactivity as a function of moderator temperature and boron concentration are presented in table 7.4.1 and fig. 7.4.1. It is seen that the moderator coefficient for 3000 ppm is still negative being -3×10^{-4} mK/C.

Table 7.4.1: Ke as a function of moderator temperature and boron concentration

°C	Water Density (g/cc)	0 ppm	1000 ppm	2000 ppm	3000 ppm	4000 ppm	10'000 ppm	20'000 ppm
280	0.765	1.17890	1.09970	1.04030	0.99333	0.94548	0.75988	0.58311
285	0.756	1.17250	1.09823	1.03977	0.98910	0.94600	0.75793	0.59582
290	0.747	1.17210	1.09520	1.03720	0.99400	0.94797	0.75912	0.59656
295	0.737	1.16970	1.09150	1.04050	0.99114	0.94650	0.76184	0.58954
300	0.727	1.16850	1.08890	1.03960	0.98790	0.94496	0.75916	0.59248
305	0.716	1.16350	1.08640	1.03720	0.98686	0.94860	0.76383	0.59364
310	0.705	1.15950	1.09370	1.03270	0.98260	0.94540	0.76474	0.59623
315	0.693	1.15620	1.09450	1.02820	0.98630	0.94280	0.76793	0.60084
320	0.681	1.15140	1.08600	1.02538	0.98300	0.94627	0.76840	0.59814
325	0.668	1.14690	1.07950	1.02821	0.97877	0.94330	0.77064	0.60546
330	0.653	1.14190	1.07310	1.02360	0.98306	0.93784	0.77197	0.60764
335	0.636	1.13580	1.06662	1.01840	0.97540	0.93965	0.77173	0.61277
340	0.618	1.12750	1.06010	1.01279	0.97006	0.93306	0.77418	0.61516

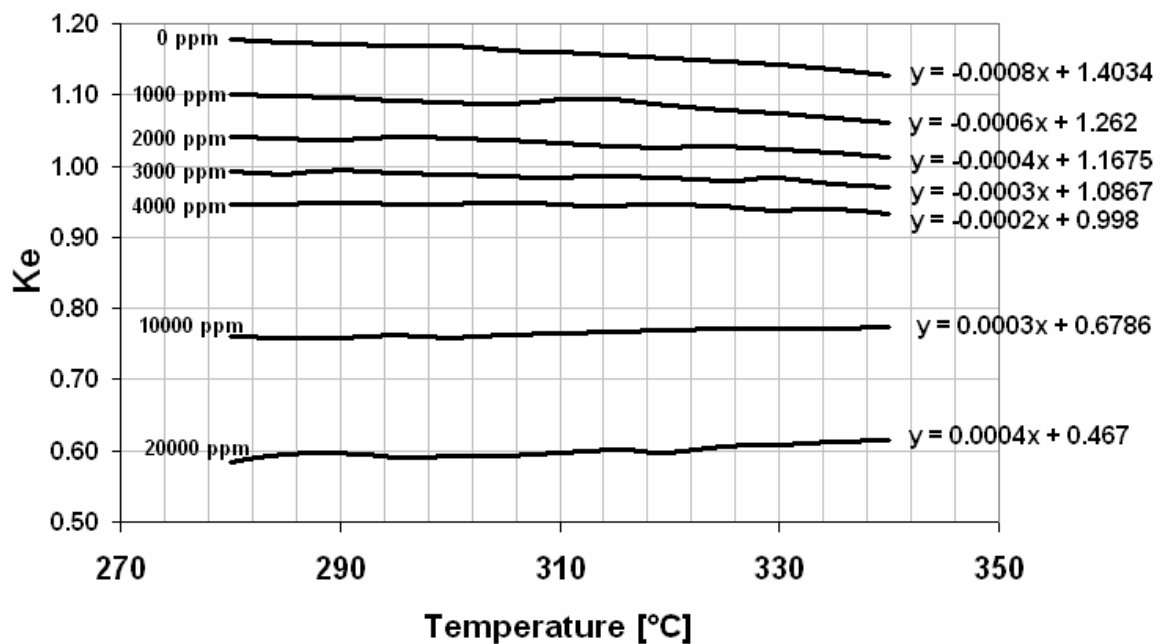


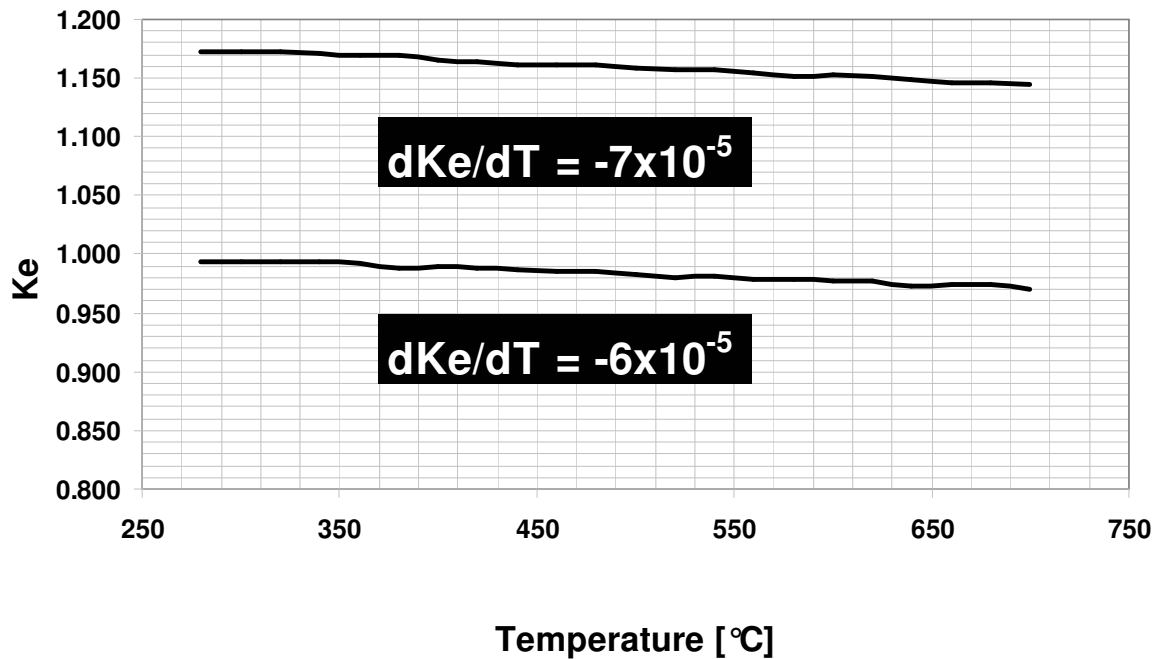
Figure 7.4.1: Ke as a function of moderator temperature and boron concentration

7.5 Doppler Effect

The values of Ke as a function of fuel temperature for 0 and 3000 ppm boron concentrations are presented in table 7.2 and fig.7.3. The Doppler coefficient for 3000 ppm boron is -6×10^{-5} mK/°C.

Table 7.5.1: K_e as a function of fuel temperature for various boron concentrations

T	0 ppm	3000 ppm	T	0 ppm	3000 ppm
280	1.1719	0.99381	500	1.1588	0.98233
300	1.1719	0.99381	520	1.1569	0.98014
320	1.1719	0.99381	540	1.1574	0.98090
340	1.1715	0.99390	560	1.1546	0.97919
360	1.1696	0.99181	580	1.1517	0.97903
380	1.1694	0.98810	600	1.1529	0.97770
400	1.1658	0.98900	620	1.1517	0.97655
420	1.1646	0.98883	640	1.1483	0.97270
440	1.1619	0.98640	660	1.1460	0.97490
460	1.1618	0.98610	680	1.1456	0.97399
480	1.1614	0.98562	700	1.1443	0.96990

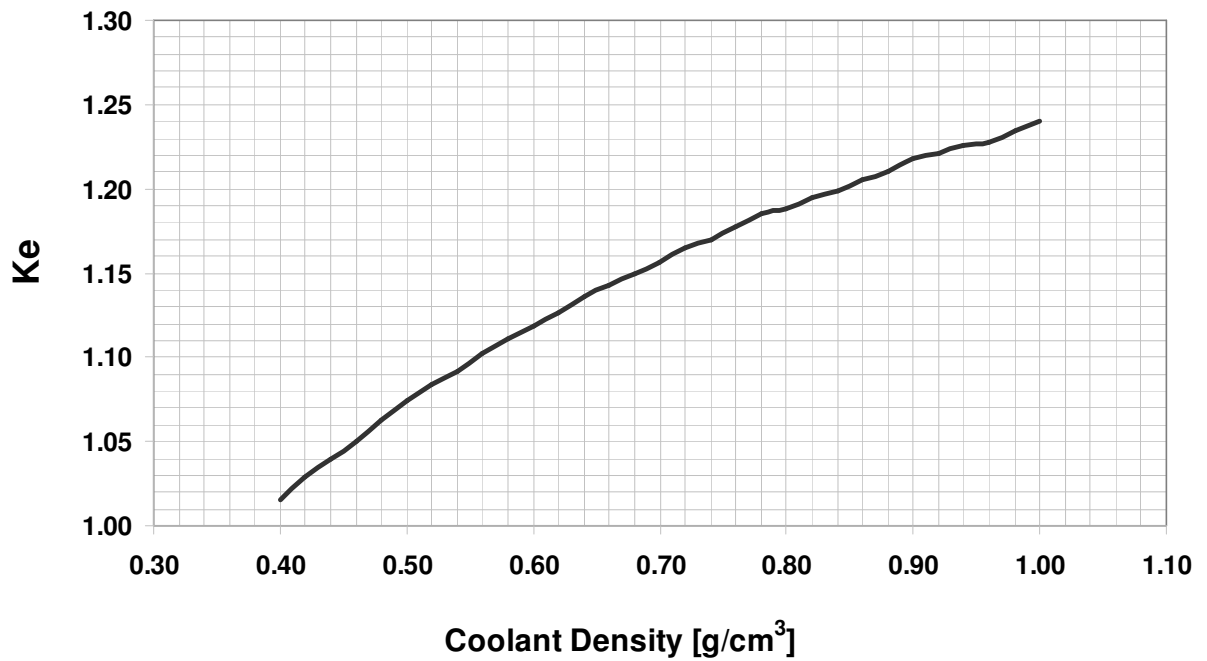
Figure 7.5.1: K_e as a function of fuel temperature

7.6 Moderator Density

The effects of moderator density variation on reactivity are presented in table 7.6.1 fig. 7.6.1, and fig.7.6.2.

Table 7.6.1: K_e as a function moderator density

ρ (g/cm ³)	K_e	$dK_e/d\rho$	ρ (g/cm ³)	K_e	$dK_e/d\rho$
0.40	1.01590	0.5589	0.72	1.16450	0.3491
0.42	1.02907	0.5457	0.74	1.17010	0.3360
0.44	1.03990	0.5326	0.76	1.17770	0.3228
0.46	1.05020	0.5195	0.78	1.18510	0.3097
0.48	1.06300	0.5064	0.80	1.18822	0.2966
0.50	1.07380	0.4933	0.82	1.19450	0.2835
0.52	1.08360	0.4802	0.84	1.19870	0.2704
0.54	1.09210	0.4671	0.86	1.20530	0.2573
0.56	1.10200	0.4540	0.88	1.21020	0.2442
0.58	1.11090	0.4409	0.90	1.21830	0.2311
0.60	1.11840	0.4277	0.92	1.22070	0.2179
0.62	1.12630	0.4146	0.94	1.22618	0.2048
0.64	1.13610	0.4015	0.96	1.22810	0.1917
0.66	1.14320	0.3884	0.98	1.23410	0.1786
0.68	1.14930	0.3753	1.00	1.23986	0.1655
0.70	1.15590	0.3622			

Figure 7.6.1: K_e as a function of moderator density

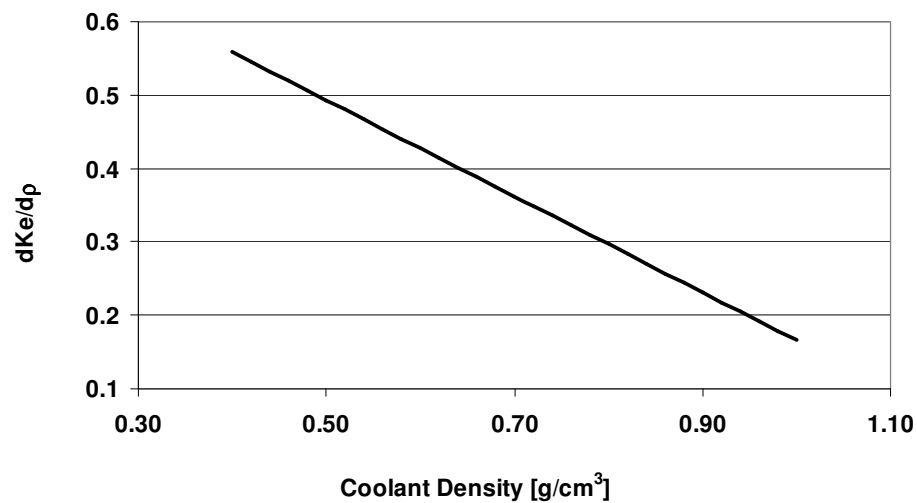


Figure 7.6.2: Sensitivity of K_e to moderator density.

8. Burnup Calculations

The Burnup calculations were made by using the SCALE5 module STARBUCS. This module allows automatic criticality analyses of spent fuel systems employing burnup credit. As a first step STARBUCS starts the burnup sequence for a depletion analysis calculation, performed using the ORIGEN-ARP module of SCALE5. The spent fuel compositions are then used to generate resonance self-shielded cross sections, which are applied in a three-dimensional criticality safety calculation using the KENO code.

The variables for the burnup-calculations were the burnup-time, the average specific power of the assembly for each cycle (POWER) and the enrichment of the core. Power density [MW/MTU] is thermal power generation per mass of uranium inside the core. Here the burnup of FBNR reactor of 218 MWt (70 MWe) are studied.

8.1 Burnup calculations

Table 8.1.1: Burnup calculation for various fuel enrichment

Days	MWD/ton	2.0%	2.5%	3.0%	3.5%	4.0%	4.5%	5.0%
0	0	0.99140	1.04433	1.08190	1.1157	1.13740	1.15772	1.17100
1	20.098	0.96608	1.01750	1.05597	1.08465	1.11490	1.13290	1.15220
2	40.196	0.96163	1.01659	1.05399	1.08368	1.10780	1.13080	1.14513
3	60.294	0.96150	1.01334	1.05270	1.08080	1.10830	1.12840	1.14700
4	80.392	0.95915	1.01310	1.05380	1.08280	1.10750	1.12840	1.14450
5	100.490	0.96022	1.01183	1.05170	1.08270	1.10890	1.12678	1.14600
6	120.588	0.95854	1.01090	1.05000	1.07840	1.10540	1.12730	1.14410
7	140.686	0.95750	1.01188	1.04938	1.08050	1.10580	1.12670	1.14356
8	160.784	0.95875	1.01082	1.04960	1.08140	1.10350	1.12695	1.14500
9	180.882	0.95760	1.00940	1.04806	1.07969	1.10450	1.12660	1.14180
10	200.980	0.95686	1.00690	1.05040	1.07960	1.10400	1.12700	1.14330
120	2411.760	0.93822	0.98520	1.02150	1.05330	1.07900	1.10130	1.11830

240	4823.520	0.90973	0.95605	0.99394	1.02532	1.05290	1.07303	1.09380
360	7235.280	0.88175	0.92595	0.96619	0.99960	1.02896	1.04935	1.07162
480	9647.040	0.85650	0.90037	0.94204	0.97234	1.00339	1.02560	1.04685
600	12058.800	0.83224	0.87824	0.91582	0.94775	0.97850	1.00270	1.02440
720	14470.560	0.81418	0.85634	0.89521	0.93004	0.95727	0.98285	1.00590
840	16882.320	0.79650	0.83989	0.87730	0.90792	0.93860	0.96344	0.98780
960	19294.080	0.78075	0.82019	0.85478	0.88997	0.92159	0.94707	0.96790
1080	21705.840	0.76510	0.80260	0.83943	0.87240	0.90160	0.92777	0.95401
1200	24117.600	0.75060	0.78796	0.82215	0.85542	0.88572	0.91170	0.93700
1320	26529.360	0.73802	0.77165	0.80770	0.83880	0.86710	0.89604	0.91990
1440	28941.120	0.72651	0.75972	0.79241	0.82321	0.85117	0.87950	0.90370
1560	31352.880	0.71327	0.74593	0.77559	0.80710	0.83770	0.86147	0.88816
1680	33764.640	0.70463	0.73457	0.76243	0.79420	0.82257	0.84940	0.87320
1800	36176.400	0.69383	0.72210	0.75213	0.78027	0.80685	0.83301	0.85942
1920	38588.160	0.68648	0.70967	0.73910	0.76564	0.79557	0.82202	0.84588
2040	40999.920	0.67710	0.70124	0.72502	0.75258	0.78055	0.80768	0.83042
2160	43411.680	0.66783	0.68944	0.71342	0.73867	0.76491	0.79008	0.81705
2200	44215.600	0.66635	0.68626	0.70742	0.73432	0.76059	0.78587	0.81098

Burnup

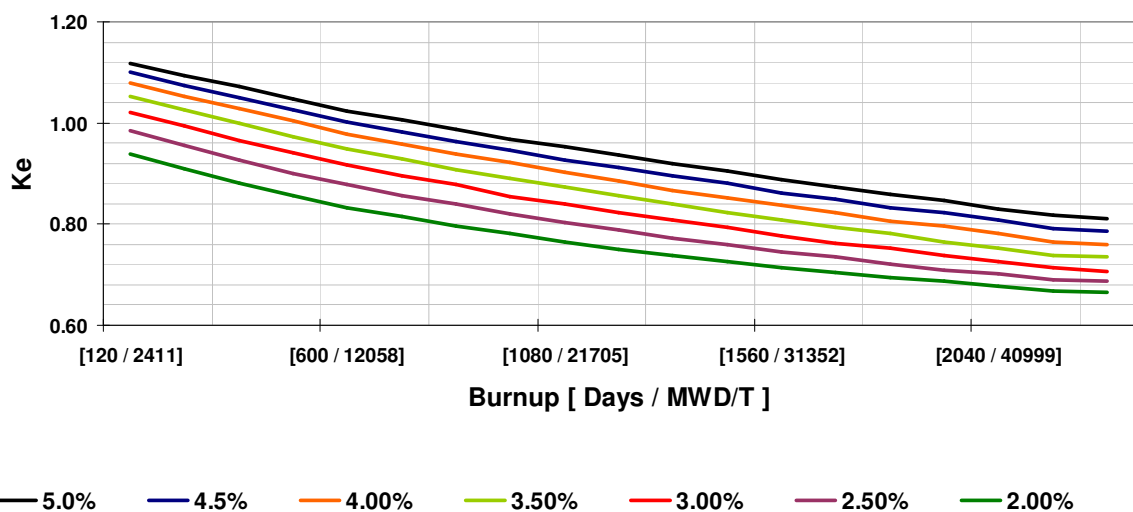


Figure 8.1.1: Burnup calculation for various fuel enrichment

It is observed that around the end of the cycle (EOC), the variation of reactivity as a function of burnup is almost linear. With such a linear assumption, the fuel lifetime as a function of enrichment are calculated as shown in table 8.1.2 and fig.8.1.2. The excess reactivity Δk_e (mK) at the beginning of the cycle (BOC) is also tabulated. The Plutonium buildup in the core at the EOC is 62 Kg and the U235 remaining in the core is 340 Kg..

Table 8.1.2: Fuel lifetime as a function of enrichment

%	5.00	4.50	4.00	3.50	3.00	2.50
Days	759	616	496	358	214	45
MWD/T	15257	12387	9975	7198	4293	904
Initial $\Delta(mKe)$	171	158	137	116	82	44

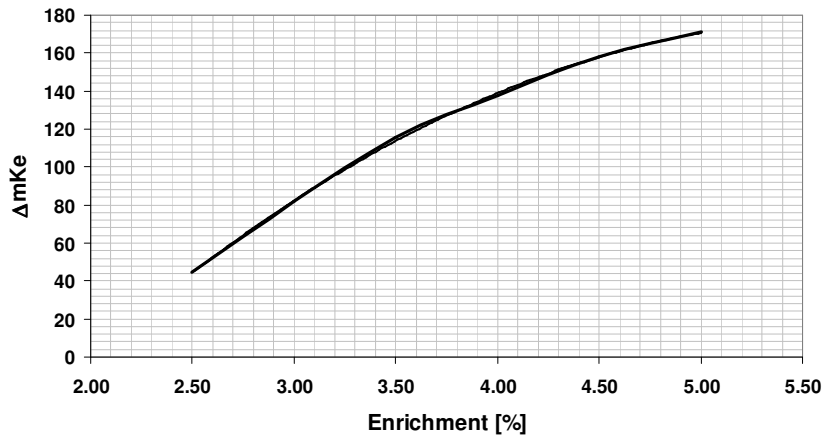


Fig. 8.1.2: Excess reactivity as a function of enrichment

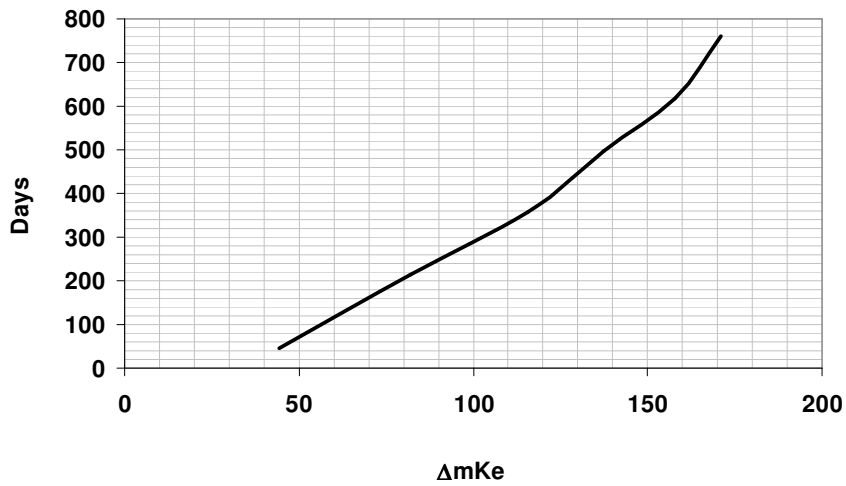


Fig. 8.1.3: Fuel lifetime as a function of initial excess reactivity

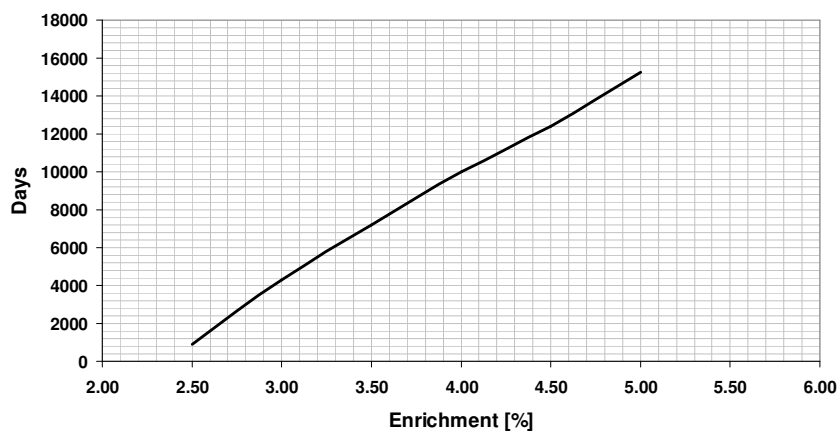


Fig. 8.1.4: fuel lifetime as a function of enrichment

Fitting the above data (y represents fuel life and x enrichment) by a linear equation results in

$$y = 280.97x - 638.9$$

It is seen that each percent of fuel enrichment contribute to 281 days [5627 MWD/T] of the fuel lifetime.

9. Reactor operation and safety

9.1 Reactor start up and shut down

To startup the reactor, the core height level limiter (CHLL) is down maintaining the core height below 30 cm where the $K_e < 0.95$ in the cold condition as seen in Table 9.1.1 and Fig. 9.1.1. Then the pump is turned on and let the coolant temperature increase to operating temperature ($\sim 308^\circ\text{C}$) due to the pump power dissipation. This will take about 20 minutes. When the coolant temperature is reached the operating temperature, then the CHLL is moved up and thus core height is increased to allow the reactor reach criticality. The expected critical height is about 200 cm. The largest effect of CHLL is 0.37 mK/cm at the BOC and decreases to 0.059 at the EOC. (see table 7.3.1). The effect of boron is 0.039 mK/ppmB at the BOC. The 200 cm height reactor with 2900 ppmB has $K_e=0.99160$ and with 2700 has $K_e=0.99981$. The uncertainty due to temperature effects justifies adoption of proposed value.

To shut down the reactor, simply the pump is turned off and the fuel elements leave the reactor core by the force of gravity and enter the fuel chamber where they remain under a highly subcritical and passively cooled condition. In this condition the accumulator valves will open automatically and the fuel chamber cooling tank becomes filled with cold water.

Table 9.1.1: K_e for standard reactor

Height	20 °C		308 °C	
	0 ppm B	2900 ppm B	0 ppm B	2900 ppm B
0	0.95980	0.80040	0.83370	0.69910
10	1.04750	0.87000	0.92150	0.78070
20	1.10610	0.92049	0.98180	0.83811
30	1.14730	0.95140	1.02060	0.87400
40	1.17320	0.97328	1.05450	0.90289
50	1.19370	0.98972	1.07950	0.92240
60	1.20880	1.00060	1.09390	0.93619
70	1.21820	1.00912	1.10760	0.94710
80	1.22870	1.01566	1.11700	0.95530
90	1.23510	1.02240	1.12430	0.96310
100	1.23750	1.02580	1.13220	0.96890
110	1.24430	1.02906	1.13560	0.97190
120	1.24970	1.03303	1.13950	0.97420
130	1.24980	1.03420	1.14430	0.97960
140	1.25300	1.03632	1.14740	0.98018
150	1.25320	1.03580	1.15110	0.98300
160	1.25760	1.03920	1.15290	0.98530
170	1.26000	1.03984	1.15270	0.98570
180	1.25900	1.04125	1.15580	0.98753
190	1.25950	1.04045	1.15770	0.98800
200	1.26250	1.04361	1.15930	0.99160
210	1.26340	1.04216	1.16060	0.99143
220	1.26380	1.04470	1.16160	0.99288
230	1.26450	1.04213	1.16230	0.99216
240	1.26500	1.04372	1.16150	0.99397
250	1.26730	1.04667	1.16360	0.99650

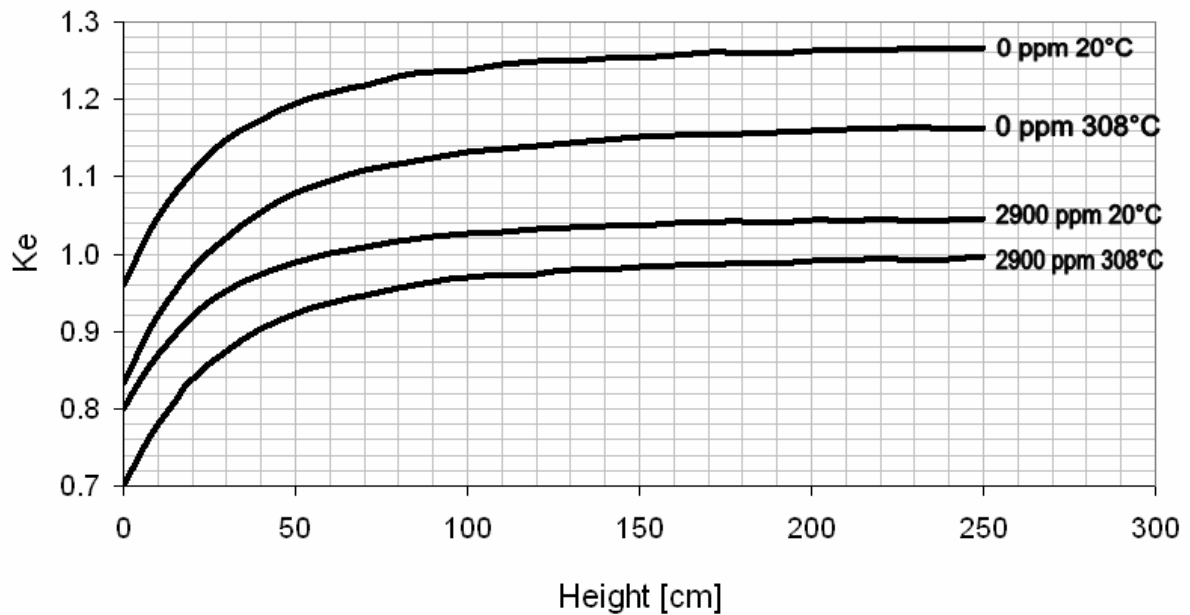


Figure 9.1.1: K_e for standard reactor.

9.2 Reactor Safety: Accident Conditions

9.2.1 The Loss of Coolant Accident (LOCA)

In the case of a LOCA, the pressure in the reactor core drops and consequently the fuel elements lose their suspend ability and fall out of the core and enter the fuel chamber where they remain under subcritical and passively cooled condition. The heat transfer calculations show that their temperature will not exceed ~ 542 °C and only less than 1 m^3 of water from accumulator is necessary to evaporate during one month of grace period.

9.2.2 The Loss of Flow Accident (LOFA)

The LOFA accident will be a more favorable accident condition than the LOCA. Again the fuel elements due to the lack of coolant flow will fall back into the fuel chamber where they remain under a subcritical and passively cooled condition. There is no need for cooling water from accumulator and the coolant in the loop will increase its temperature by only less than 1 °C.

9.2.3 The Loss of Power Accident

The loss of power simply shuts down the pump and the reactor condition will be equivalent to a LOFA case.

9.2.4 The Loss of Turbine Load or Secondary Loop Break Accident

The temperature of the cold leg of the pump increases and thus the control system shuts down the pump. Also the bubbles formed in the core decrease the moderator density thus due to the negative moderator coefficient, ($- 350 \text{ mK}/(\text{g}/\text{cm}^3)$) as seen in Table 7.6.1, the reactor becomes subcritical.

9.2.5 The Terrorist Attack

The worst condition that any terrorist action can produce will be similar to the LOCA condition. Only what is needed is to protect the fuel chamber within a robust structure.

10. Plutonium Utilization

The reactor is assumed to be fuelled by the plutonium coming from the reprocessing of FBNR spent fuel after 840 days of burnup. The fuel is thus composed of 95% U-238 and 5% Pu with isotopic composition shown in table 10.1.

Table 10.1: Composition of Pu isotopes in fresh fuel

Isótope	%
238	0.334
239	78.584
240	13.672
241	6.712
242	0.698
TOTAL	100.000

The calculated K_e as a function of core height and the percent Pu mixture in the fuel are presented in table 10.2 and Fig. 10.1. Table 10.3 and Fig. 10.2 shows a comparison between uranium and plutonium fuelled reactor in regards to the enrichment effects.

Table 10.2: K_e as a function of height and enrichment

Height	Plutonium		Uranium		Height	Plutonium		Uranium	
	2.2%	5.0%	2.2%	5.0%		2.2%	5.0%	2.2%	5.0%
10	0.77110	0.82330	0.78466	0.93670	140	0.94688	0.99330	1.00490	1.16330
20	0.81490	0.86890	0.84200	0.99860	150	0.95209	0.99443	1.00814	1.16380
30	0.84940	0.90120	0.88660	1.04060	160	0.95270	0.99760	1.00760	1.16670
40	0.87600	0.92530	0.91580	1.07120	170	0.95387	0.99830	1.01079	1.17040
50	0.89490	0.94010	0.93740	1.09140	180	0.95316	0.99960	1.01280	1.17073
60	0.90671	0.95270	0.95480	1.10970	190	0.95480	0.99960	1.01340	1.17202
70	0.91570	0.96330	0.96595	1.12270	200	0.95590	1.00081	1.01410	1.17370
80	0.92350	0.97200	0.97500	1.13350	210	0.95790	1.00450	1.01520	1.17470
90	0.93080	0.97674	0.98325	1.14080	220	0.95860	1.00473	1.01530	1.17480
100	0.93621	0.98160	0.99000	1.14650	230	0.95674	1.00400	1.01579	1.17640
110	0.94070	0.98300	0.99519	1.15100	240	0.96176	1.00370	1.01816	1.17610
120	0.94400	0.98720	0.99850	1.15600	250	0.95958	1.00580	1.01920	1.17730
130	0.94407	0.99180	1.00030	1.15860					

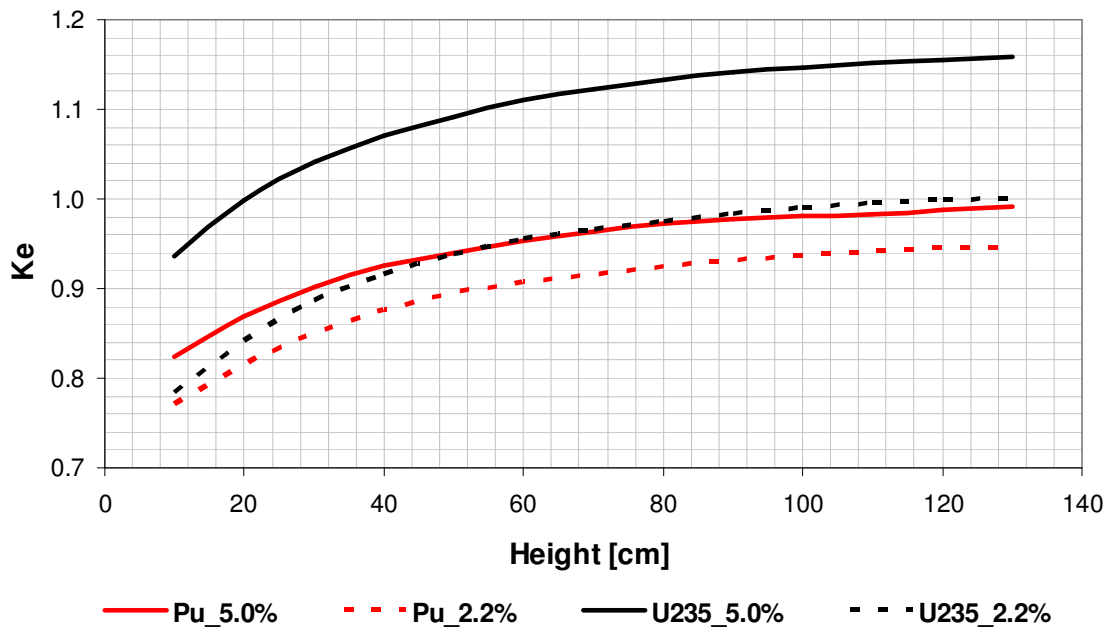


Figure 10.1: Ke as a function of core height

Table 10.3: Comparison of U vs. Pu fuel.

Enrichment	Ke_U	Ke PuO ₂	Enrichment	Ke_U	Ke PuO ₂
0	0.06823	0.06821	10	1.26310	1.05800
1	0.79748	0.87650	11	1.27580	1.06583
2	0.99140	0.95170	12	1.28510	1.07730
3	1.08190	0.97690	13	1.29280	1.09010
4	1.13740	0.98919	14	1.30280	1.09920
5	1.17100	1.00081	15	1.30870	1.11346
6	1.19910	1.01231	16	1.31480	1.12280
7	1.22040	1.02464	17	1.32490	1.13660
8	1.23660	1.03510	18	1.33150	1.14500
9	1.25250	1.04670	19	1.33780	1.15745

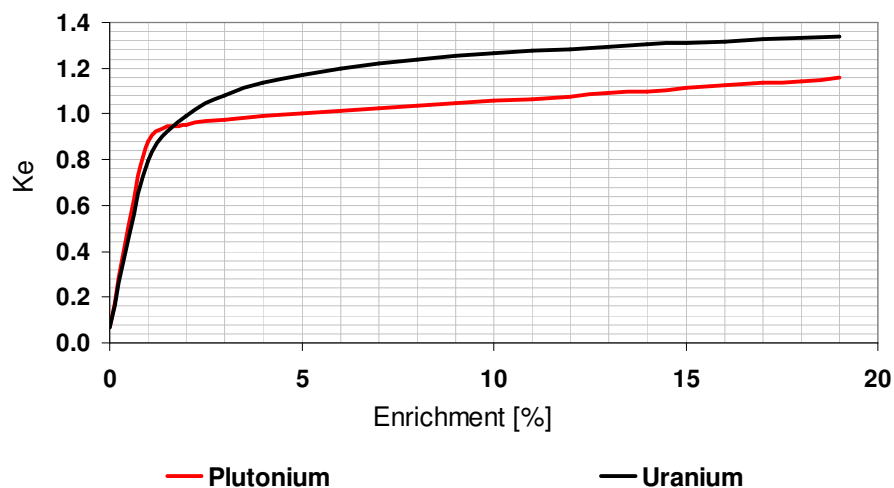


Figure 10.2: Comparison of uranium and plutonium fuelled reactor

11. Conclusions

The preliminary neutronics calculations show that behavior of the FBNR is similar to that of a conventional PWR. The core lifetime can be as long as the customer wishes, should he be ready to pay for the higher enrichment fuel than the commercially available (5%). In practice, this is not necessary as the fuel chamber that is fuelled in the factory can easily be changed. The reactor will require a change of fuel chamber once every 800 days (2.2 years) where burnup is 15300 MWD/T. Each additional percent increase in enrichment results in additional 281 days of core life. The refueling involves the disconnecting and connecting of a less than 5 m³ volume fuel chamber to the reactor by a flange that is sealed and inspected by the safeguard authorities.

The calculations show that all the reactivity coefficients of the reactor are negative resulting in safe operation of the reactor (Table 11.1). It is seen that the reactivity of the reactor can be controlled and adjusted by the manipulation of a screw type core height level limiter (CHLL) and changing the boron concentration without the need for utilizing control rods. At the beginning of cycle (BOC) the boron concentration is 2900 ppm and boron sensitivity is 0.039 mK/ppmB. The maximum CHLL sensitivity is 0.37 mK/cm.

It is seen that the FBNR is an inherently safe nuclear reactor.

Table 11.1: Reactor parameters

	Beginning of Cycle (BOC)	End of Cycle (EOC)
Moderator Coefficient (mK/ °C)	-3×10^{-4}	-8×10^{-4}
Doppler Coefficient (mK/C)	-6×10^{-5}	-7×10^{-5}
Core height level limiter (CHLL) Sensitivity (mK/cm)	0.370	0.059
Boron Sensitivity (mK/ppm)	0.039	0.080

12. References

- [1] Sefidvash, F., "Conceptual Design of the Fixed Bed Nuclear Reactor (FBNR) Concept", IAEA Year 2005 and 2006 Reports - IAEA Research Contract No. 12960/Regular Budget Fund (RBF).
- [2] Sefidvash, F., "Fixed Bed Nuclear Reactor Concept", Innovative small and medium sized reactors: Design features, safety approaches and R&D trends, IAEA-TECDOC-1451, May 2005, p. 193-202
- [3] Sefidvash, F., "Fixed bed suspended core nuclear reactor concept", Innovative Technologies for Nuclear fuel Cycles and Nuclear Power, Proceedings of International Conference held in Vienna 23-26 June 2003, p. 463-465
- [4] FBNR site: www.rcgg.ufrgs.br/fbnr.htm
- [5] Takashi Hirayama; "Benchmark results of various particle fuels For small reactors without on-site refueling", PHYTRA1: First International Conference on Physics and

Technology of Reactors and Applications. Marrakech (Morocco), March 14-16, 2007, GMTR (2007)

[6] F.Briesmeister, Ed., "MCNP-A General Monte Carlo N-particle Transport Code Version 4C", LA-12625-M, (2000).

13. Acknowledgement

The authors would like to thank the IAEA for its continuing financial support under the Research Contract No. 12960/R2.